AN ATOMIC BEAM METHOD
FOR MEASURING ABSOLUTE f-VALUES

Thesis by

Milford Hall Davis

In Partial Fulfillment of the Requirements

for the Degree of

Doctor of Philosophy

California Institute of Technology

Pasadena, California

1955

ACKNOWLEDGEMENTS

This experiment is part of a comprehensive research program on f-values which is being carried out under the direction of Dr. Robert B. King. It is a pleasure to acknowledge his generous help and encouragement both in the experimental work and in the preparation of this thesis.

Dr. Paul M. Routly contributed significantly to the final design of the atomic beam apparatus. Much of the credit for the operative success of the apparatus should go to Mr. Glen Sligh in whose able hands most of the difficult construction work was placed.

I wish to thank Mr. Graydon Bell for his assistance in the final stages of the experiment and Mr. Albert R. Hibbs for his encouragement and for his many helpful suggestions.

I am grateful to the California Research Corporation for a fellowship during the years 1951-1953.

ABSTRACT

Very few absolute oscillator strengths (f-values) are known for lines in complex spectra; little confidence can be placed in most of the results which have been reported. In an effort to remedy this situation an atomic beam apparatus was constructed and used for the experimental determination of the absolute f-values of resonance lines in the Fe I, Cr I, Mn I, and Cu I spectra.

The theory of the formation of absorption lines when light from a source of continuous radiation passes through an atomic beam was developed and is presented in some detail. The atomic beam apparatus, devices for temperature measurement and control, and methods for determining the density of atoms in the atomic beam are described.

A discrepancy was noticed between the predicted and observed variation of the total absorption for a particular line with the number of absorbing atoms. The observed relation was used as an auxiliary means for the determination of absolute f-values in a manner which is described at length. Since the resulting f-values differ somewhat from those calculated from the data on the basis of the atomic beam theory, both sets of results are reported. Recommendations are made for further research to resolve this problem.

TABLE OF CONTENTS

TABLES

FIGURES

I. INTRODUCTION

A. Background

When light from a source of continuous radiation passes through a layer of atoms in a vapor, absorption and dispersion occur for frequencies near the atomic resonant frequencies. According to the classical electron theory the magnitude of either phenomenon near a resonance depends upon $\mathcal{N}$, the number of "equivalent classical oscillators" per unit volume which participate. $\mathcal{N}$ is related to N, the number of atoms per unit volume which are active in the absorption process near a particular resonance, by the relation

$$\mathcal{N} = Nf. \qquad (1.1)$$

The factor f is the number of equivalent classical oscillators per atom, the so-called oscillator strength or f-value of the transition involved.

Although the wavelengths of many thousands of spectral lines have been measured with great precision and a large number have been classified according to the atomic transition involved, f-values are known in comparatively few cases. The principal motivation behind research on f-values arises from their importance in astrophysics. The abundances of the various elements in stellar objects can be calculated from observed spectral line strengths and inferences can be made regarding the excitation temperatures of the atoms involved if the f-values are known. King[1], Sandage and Hill[2], and Claas [3] give examples of this sort of calculation. The elements of the "iron-group", from Sc to Cu in the periodic table, are particularly important in astrophysics and it is with

this group of elements that we shall be principally concerned here.

A complete theory of the formation of absorption lines has been developed using the methods of quantum mechanics. If the final equations are compared with the corresponding ones of the classical electron theory it is found that the f-value defined by Eq. (1.1) is given quantum mechanically by

$$f = \frac{8\pi^2 m \nu}{3e^2 h} |\mathfrak{m}|^2 . \qquad (1.2)$$

In Eq. (1.2), as throughout this paper, e and m are the charge and mass of the electron, h is Planck's constant, ν is the frequency of the transition, and $\mathfrak{m}$ is the matrix element of the electric dipole moment between the two states involved. (See Slater[4], Chapter 4.) In principle, therefore, f-values can be calculated if the wave functions for the two states are known. Extensive calculations have indeed been made for H, He, and a number of hydrogen-like atoms and ions. Bates and Damgaard[5] give a thorough discussion of what can be done in more complicated cases and a tabulation of the results of f-value calculations for some eighteen atoms and ions is given in Landolt-Börnstein.[6] Sometimes f-values can be estimated from the Thomas-Kuhn sum rule which states that for a single electron system the sum of the f-values for all transitions is unity. (See Aller[7], pp. 131-135.) Unsöld[8] has made use of f-values estimated in this manner in order to complete his table of solar abundances but the results are probably not very reliable for atoms with complex spectra.

For all but the simplest atomic systems f-values are undoubtedly best determined by experiment. Mitchell and Zemansky[9] give a summary

of the methods which have been used. Recent experimental determinations of f-values have usually been made either (1) by measuring emission line strengths in arc spectra (Schuttevaer and Smit[10], for example), or (2) by measuring the strengths of absorption lines formed under known conditions (King and King[11]). Both approaches give only relative f-values unless N of Eq. (1.1) can be determined. However, relative f-values are useful to the astrophysicist and eventual determination of the absolute f-value for any one line puts the entire set on an absolute basis.

In order to determine absolute f-values for Cu I King and Stockberger[12] measured the strengths of absorption lines produced by vapor of the metal in equilibrium with the solid in a quartz absorption cell. They used the vapor pressures given by Kelley [13] to convert their data to absolute values. King[14] later determined the absolute f-values of Fe I in the same manner and Estabrook[15, 16] applied the method to Cr I and Ni I. The absolute f-values obtained by this method are only as reliable as the vapor pressure data on which they are based. Unfortunately, even today the vapor pressure data for these fairly refractory metals are of questionable accuracy in most cases.

The atomic beam method was developed in an effort to get away from the necessity of using vapor pressure data. Kopfermann and Wessel[17] measured the absorption by a beam of Fe atoms of the Fe I resonance lines from a hollow cathode source. The density of the absorbing atoms was measured directly by means of a microbalance mounted inside the vacuum system, thus avoiding dependence upon vapor pressure measurements. The absolute f-values obtained by Kopfermann and Wessel for Fe I, however,

were larger than those of King[14] by a factor of 3.

B. The Present Experiment

The present experiment was undertaken to redetermine the absolute f-values of Fe I and to extend these measurements to include other elements of astrophysical interest. An atomic beam method similar to that of Kopfermann and Wessel was used. In outline the experiment was conducted as follows: The element under investigation was evaporated in an oven inside a vacuum chamber and a fan-shaped beam of atoms was formed. Some of these atoms were caught either on light aluminum or mica sheets which were weighed before and after a run, or on a light aluminum pan attached to a quartz helix suspended inside the vacuum chamber. The temperature of the source was measured by means of an optical pyrometer. Light from a high pressure mercury arc passed through the atomic beam and was focused on the slit of a 21 ft grating spectrograph. Figure 1 shows a diagram of the experimental set-up. The spectra were photographed using high contrast fine-grain emulsion plates and the total absorptions of the lines were measured from microphotometer tracings of the plates.

Absolute f-values were obtained for Fe I, Cr I, Mn I, and Cu I. The results are discussed in the sections devoted to the individual elements.

The usual theory of the formation of absorption lines applies only to experiments in which light from a source of continuous radiation passes through a layer of gas of uniform density which is in thermal equilibrium. It is presented in detail in many texts. (For example, comprehensive treatments are to be found in Mitchell and Zemansky[9] and Aller[7].)

Some modification of this theory is necessary if it is to be applied to the formation of absorption lines by a beam of atoms since this is a situation in which both the density and the velocity distribution function of the atoms vary from point to point in space. This modified theory is developed in detail in the following section.

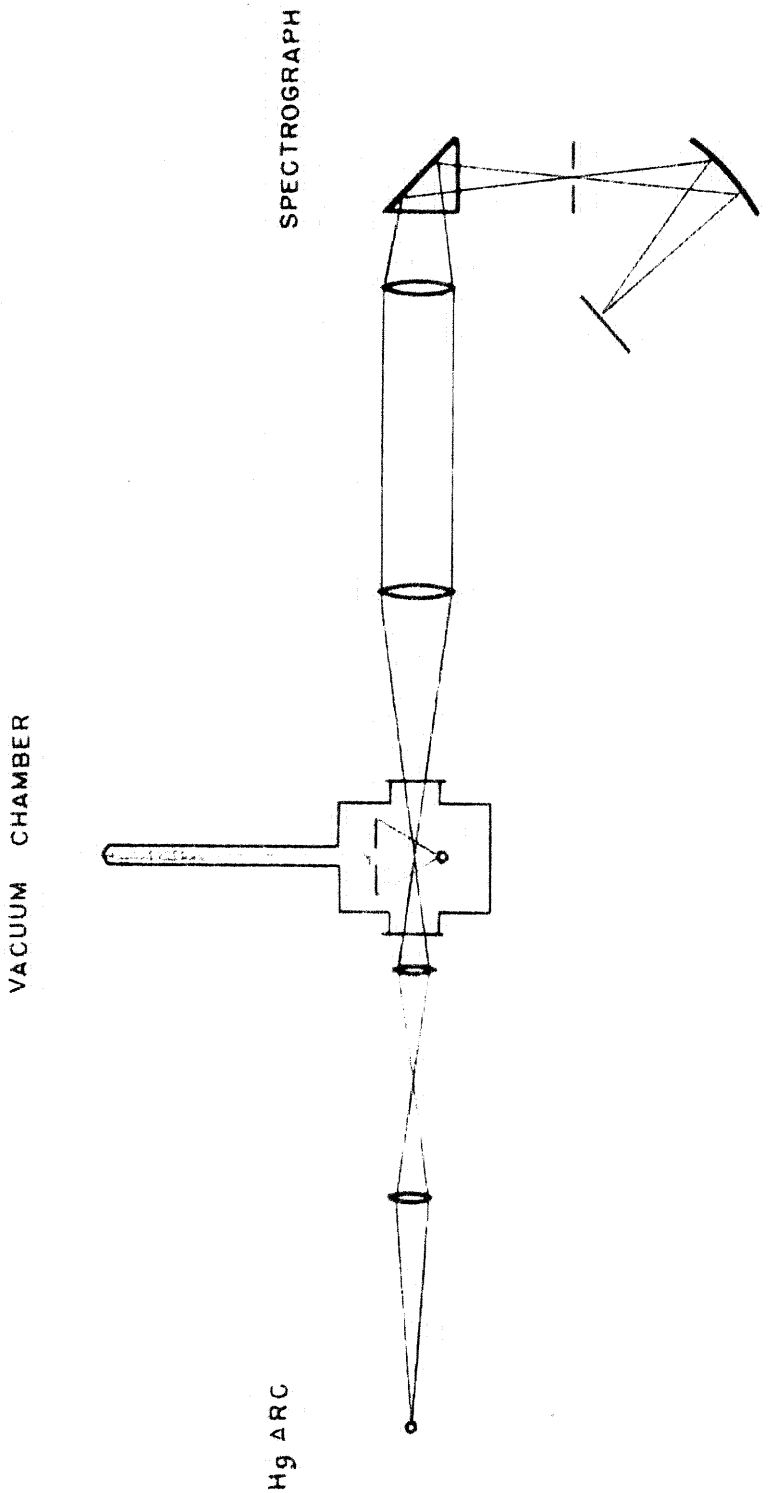

FIG. 1

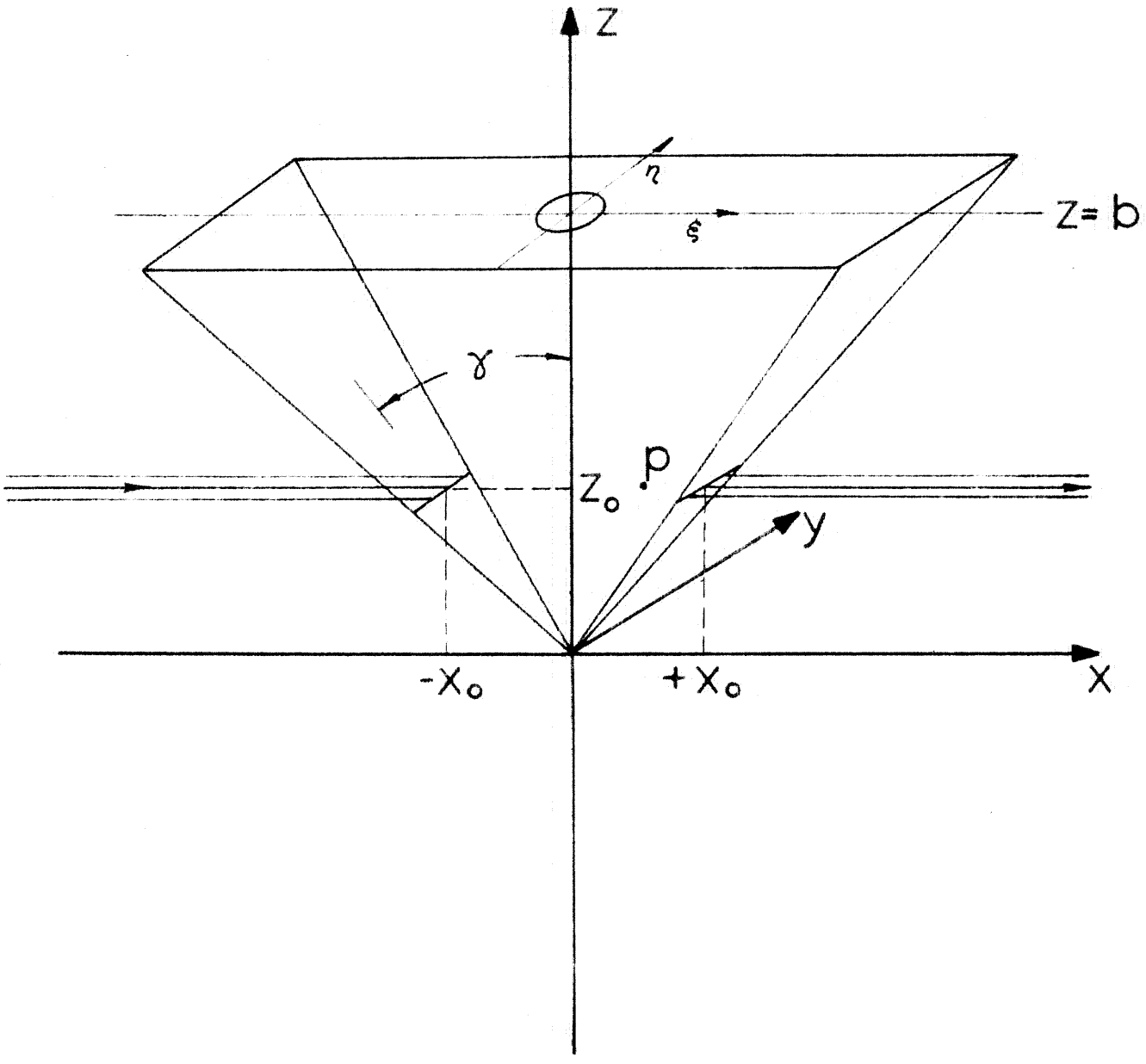

FIG. 2

II. THEORY

A. Assumptions

In the atomic beam method of determining f-values the atoms which produce the absorption lines are emitted from a source of small area within a vacuum chamber. They pass through a defining slot which is large compared to the source and so form a fan-shaped beam. (See Fig. 2.) In order to simplify the development the following assumptions will be made:

(1) It will be assumed that the density and velocity distribution functions for atoms in the beam may be derived from the equations of the kinetic theory of gases which describe molecular effusion.

True effusive flow occurs only when the dimensions of the source (if it is an orifice) are small compared to the mean free path of the gas atoms. (Kennard[18] discusses this point.) The conditions which prevailed in this experiment were usually fairly far from this ideal. For each element used there was a certain minimum flux of atoms into the atomic beam for which absorption lines would be observed. In order to achieve this minimum flux of atoms from a small orifice it was necessary to operate at temperatures so high that the mean free path of the atoms inside the oven was about 1/50 the diameter of the orifice. However, in several cases the orifice hole was made so large compared to the other dimensions of the oven that the source of atoms was effectively a free metal surface. In these cases it was possible to achieve the required minimum flux of atoms at temperatures for which the mean free path of the atoms was of the same order of magnitude as the smallest linear

dimension of the evaporating area. Since the values obtained under these two conditions checked within experimental error it was concluded that possible departures from effusive flow were not significant for this experiment. This remains a somewhat questionable point, however. It is discussed further in the section on the interpretation of the results. The actual distribution of atoms in the beam from a small orifice was obtained and found to agree within a few percent with the distribution predicted by the kinetic theory. This experiment is described in the Appendix, Section VI.

(2) The source area will be assumed sufficiently small that the atoms may be considered to emanate from a point which will be taken as the origin of coordinates (see Fig. 2). Also the light beam will be considered to be a pencil of rays of negligible width and thickness passing through the center of the atomic beam.

The effects of both the finite area of the source and the finite extension of the light beam can be calculated, though the resulting expressions are rather cumbersome. In this experiment these factors were estimated to affect the final f-values by less than one percent.

(3) It will be assumed that the effect of collisions of atoms in the beam with residual gas molecules can be neglected.

The residual gas pressure in the vacuum chamber as measured with an ionization guage was always below 10^{-4} mm-Hg during runs and was usually in the range $2\text{-}6 \times 10^{-5}$ mm-Hg. At these pressures only a few percent of the atoms will collide with residual gas molecules as they traverse the vacuum chamber from the source to the point where they are collected. It seems reasonable, therefore, to believe that the effect on the measured f-values of scattering by residual gas molecules will be small.

(4) It will be assumed that all atoms in the atomic beam which strike a cool surface stick there.

When the shutter is first opened and the atomic beam allowed to strike the pan attached to the quartz helix a "kick" is observed. This kick is due to the force which results from the momentum transfer from the atomic beam to the balance pan. The force can be directly measured from the observed kick of the helix, since its spring constant is known. The force can also be calculated since it is equal to the depositing rate multiplied by the mean velocity of the atoms provided no reflection occurs. It was found that the observed and calculated momenta agreed within experimental error so it was concluded that reflection or re-evaporation of atoms did not constitute an important source of error. (A more detailed discussion of this subject is given in Section II-E.)

Having now stated the assumptions which will be used we will proceed with the theoretical development.

B. Theory

When light of intensity I_ν at frequency ν passes through a thin layer of gas the fraction which is absorbed is given by

$$\frac{\Delta I_\nu}{I_\nu} = \alpha_\nu N(\Delta x) \qquad (2.1)$$

where Δx is the thickness of the gas layer. Since the theory to be developed here concerns the formation of absorption lines by the gas, the absorption will be considered to be due to the presence of an absorption line centered at ν_o. As in Eq. (1.1) N is the number of atoms per unit volume capable of absorbing frequency ν and α_ν is the absorption coef-

ficient per atom. If thermal motions in the gas are neglected α is given by the Weisskopf-Wigner relation:

$$\alpha_\nu = \frac{\pi e^2}{mc} f \frac{\Gamma}{4\pi^2} \left[(\nu - \nu_o)^2 + \left(\frac{\Gamma}{4\pi}\right)^2 \right]^{-1} . \qquad (2.2)$$

where Γ is the natural damping constant of the line and f is the oscillator strength (see Aller[7] Chapter 5, Eq. (65)).

Although the actual line shape is determined by Γ, the integral of α_ν over all frequencies is independent of Γ :

$$\int_o^\infty \alpha_\nu \, d\nu = \frac{\pi e^2}{mc} f. \qquad (2.3)^*$$

This equation must hold no matter what phenomena affect the observed line shape in a particular experimental situation provided N is not appreciably altered by the absorption. (Mitchell and Zemansky[9] Chapter 3, Section 1a, derive Eq. (2.3) from a somewhat different point of view and discuss its applicability.)

Figure 2 shows a simplified diagram of the atomic beam. The positive x direction is the direction of the light beam; the z axis is the axis of the atomic beam. The number of atoms per second which enter solid angle $d\Omega$ with speeds between v and v + dv is given by Kennard[18] as:

$$K \cos\theta \, \beta^3 v^3 e^{-\beta^2 v^2} \, d v \, d\Omega . \qquad (2.4a)$$

θ is the angle that the axis of the solid angle $d\Omega$ makes with the z axis, $\beta = \sqrt{\frac{M}{2RT}}$, where R is the gas constant per mole, M is the atomic

---

*In c.g.s. units $\frac{\pi e^2}{mc}$ has the value 2.64×10^{-2} cm^2/sec.

weight, and T is the absolute temperature.

At a point P in the atomic beam (the x coordinate of P is positive) there are

$$N_v dv = K \frac{\cos\theta}{r^2} \beta^3 v^2 e^{-\beta^2 v^2} dv \qquad (2.4b)$$

atoms per unit volume with speeds between v and v + dv. The total number of atoms per unit volume is

$$\int_0^\infty N_v dv = K \frac{\sqrt{\pi}}{4} \frac{\cos\theta}{r^2} = K \frac{\sqrt{\pi}}{4} \left(\frac{z}{r^3}\right). \qquad (2.5)$$

In terms of the component of velocity in the x direction, u, and expressed in Cartesian coordinates, Eq. (2.4b) may be rewritten

$$N_u du = K \beta^3 \left(\frac{z}{x^3}\right) u^2 e^{-\beta^2 u^2} \left(\frac{r}{x}\right)^2 du \qquad (2.6)$$

where $r^2 = x^2 + y^2 + z^2$.

If an atom at rest will absorb light of frequency ν, when moving with velocity u away from the light source it will absorb frequency $\nu' = \nu \left(1 + \frac{u}{c}\right) = \nu + \delta$ (the doppler shift).

So $$u = \delta \left(\frac{c}{\nu}\right). \qquad (2.7)$$

The probability that an atom at P (which at rest will absorb frequency ν) is moving with a velocity component in the x direction such that the frequency it will absorb is shifted by an amount $\delta > 0$ is obtained by using (2.7) and dividing Eq. (2.6) by the total number of atoms per unit volume. This probability is therefore given by

$$P_\delta d\delta = \frac{4}{\sqrt{\pi}\,\Delta\nu_D}\left(\frac{r}{x}\right)^3 \left(\frac{\delta}{\Delta\nu_D}\right)^2 \exp\left[-\left(\frac{r\,\delta}{x\Delta\nu_D}\right)^2\right] d\delta, \qquad (2.8)$$

where $\Delta\nu_D = \frac{\nu}{\beta c}$.

For a moving atom the central frequency of the absorption line is not ν_o but $\nu_o + \delta$. The probability of the shift δ is given by $P_\delta d\delta$. Therefore, the absorption coefficient per atom, taking into account the motions of the atoms, is

$$\alpha = \frac{\pi e^2}{mc} f \left(\frac{\Gamma}{4\pi^2}\right) \int_0^\infty \frac{P_\delta d\delta}{(\nu_o + \delta - \nu)^2 + \left(\frac{\Gamma}{4\pi}\right)^2}. \qquad (2.9)$$

In order to simplify this expression the following substitutions will be made:

$$\omega = \frac{\nu - \nu_o}{\Delta\nu_D}$$

$$a = \frac{\Gamma}{4\pi\Delta\nu_D}$$

$$\eta = \frac{\delta}{\Delta\nu_D}$$

Then

$$\alpha_\nu = k_o f \frac{4a}{\pi} \int_0^\infty \frac{\left(\frac{r}{x}\right)^3 \eta^2 \exp\left[-\left(\frac{r\eta}{x}\right)^2\right] d\eta}{a^2 + (\omega - \eta)^2} \qquad (2.10)$$

where $k_o = \frac{\sqrt{\pi}\, e^2}{mc\Delta\nu_D}$.

The probability of a frequency shift δ given by Eq. (2.8) is valid only for positive values of δ. The probability of a negative frequency

shift is zero since at point P in the atomic beam all the atoms are moving away from the light source and so all experience positive frequency shifts. This effect was taken into account in Eq. (2.9) by integrating only over positive values of δ. Similarly only negative frequency shifts occur at points in the region $x < 0$.

When light of a given frequency passes through the atomic beam from $-x_o$ to $+x_o$ (Fig. 2), the transmitted intensity is

$$I_\nu(x_o) = I_\nu(-x_o) \exp\left[-\int_{-x_o}^{x_o} N(x)\alpha_\nu(x)\,dx\right]. \qquad (2.11)$$

In the region $x > 0$,

$$N(x)\alpha_\nu(x) = \frac{2Cz^2a}{\pi x^3}\int_0^\infty \frac{\eta^2 e^{-\eta^2\left(1+\frac{z^2}{x^2}\right)}}{a^2+(\omega-\eta)^2}\,d\eta, \qquad (2.12a)$$

where $C = \dfrac{\sqrt{\pi}\,k_o\,f\,K}{2z}$, and, as before, $\omega = \dfrac{\nu-\nu_o}{\Delta\nu_D}$. For $x < 0$, where the the doppler frequency shifts are negative,

$$N(x)\alpha_\nu(x) = \frac{-2Cz^2a}{\pi x^3}\int_0^\infty \frac{\eta^2 e^{-\eta^2\left(1+\frac{z^2}{x^2}\right)}}{a^2+(\omega+\eta)^2}\,d\eta. \qquad (2.12b)$$

Hence,

$$\int_{-x_o}^{x_o} N(x)\alpha_\nu(x)\,dx = \frac{2Cz^2a}{\pi}\int_0^\infty\left[\frac{1}{a^2+(\omega-\eta)^2}+\frac{1}{a^2+(\omega+\eta)^2}\right]\cdot \left[\int_0^{x_o}\frac{\eta^2}{x^3}e^{-\eta^2\left(1+\frac{z^2}{x^2}\right)}\,dx\right]d\eta \qquad (2.13)$$

$$= \frac{Ca}{\pi} \int_0^{\infty} \left(\frac{1}{a^2 + (\omega-\eta)^2} + \frac{1}{a^2 + (\omega+\eta)^2} \right) e^{-\eta^2 \csc^2\gamma} d\eta. \qquad (2.14)$$

γ is the half-angle of the atomic beam, so $\csc^2\gamma = 1 + \frac{z^2}{x_o^2}$.

If an absorption line is sufficiently weak (a criterion will be given later on) and the value of $\underline{a}$ for the line is small, then the line shape is essentially determined entirely by the doppler effect and no appreciable error will result if $\underline{a}$ is considered to be vanishingly small. For resonance lines, such as are of interest here, $\underline{a}$ is of the order of 0.01. So, provided the total absorption is not too large, very little error will result if the limiting value for $\underline{a} \longrightarrow 0$ is used in the evaluation of the integral in Eq. (2.14).

In the limit, for $\underline{a} \longrightarrow 0$,

$$\int_{-x_o}^{x_o} N(x) \alpha_\nu(x) dx = C\, e^{-\omega^2 \csc^2 \gamma}. \qquad (2.15)$$

The method by which the result given in Eq. (2.15) may be obtained from Eq. (2.14) is given by Mitchell and Zemansky[9], pp. 320, 321.

The total absorption of one absorption line is defined by the relation

$$W = \int_0^{\infty} \frac{I_\lambda(-x_o) - I_\lambda(x_o)}{I_\lambda(-x_o)} d\lambda$$

which is called the "equivalent width" of the line if λ is in Angstrom units, or by

$$W = \Delta\lambda_D \int_{-\infty}^{\infty} \frac{I_\omega\,(-x_o) - I_\omega\,(x_o)}{I_\omega\,(-x_o)}\, d\omega \qquad (2.16)$$

where $\Delta\lambda_D = \frac{\lambda_o}{c}\sqrt{\frac{2RT}{M}}$ is the so-called doppler width of the line. Note that ω is a dimensionless variable defined alternatively by $\omega = \frac{\lambda - \lambda_o}{\Delta\lambda_D}$ or $\omega = \frac{\nu - \nu_o}{\Delta\nu_D}$. So, for the atomic beam case, from Eqs. (2.14) and (2.15), where I_ω is assumed to be constant over the line,

$$\frac{W}{\Delta\lambda_D} = \int_{-\infty}^{\infty} \left[1 - \exp\left(-C\, e^{-\omega^2 \csc^2\gamma}\right)\right] d\omega. \qquad (2.17)$$

This expression is readily integrated by expanding the exponential in a power series which is then integrated term by term to give

$$\frac{W}{(\Delta\lambda_D)'} = \frac{W}{(\Delta\lambda_D \sin\gamma)} = \sqrt{\pi} \sum_{n=1}^{\infty} \frac{C^n\,(-1)^{n+1}}{n!\,\sqrt{n}}\,. \qquad (2.18)$$

A table of values of C as a function of $\frac{W}{(\Delta\lambda_D)'}$ was calculated for C from 0.034 to 10. The relationship is roughly linear for $\frac{W}{(\Delta\lambda_D)'} < 0.6$, then between 1.0 and 3.0 the slope of the function becomes progressively smaller until for $\frac{W}{(\Delta\lambda_D)'} = 3.0$ a change of 10 percent in $\frac{W}{(\Delta\lambda_D)'}$ corresponds to a change of 40 percent in C. Mitchell and Zemansky[9] give a graph of the function over a large range of both variables.* Equation (2.18) shows that in order to obtain f-values of reasonable accuracy from measured equivalent widths it is clearly necessary that sin γ be as close to unity as possible. Physically this means that the atomic beam apparatus should be designed so that the angular spread of the beam is large. If one insist that sin γ be greater than 0.5, then γ must be at least 30°. In the experi-

*See also Figs. 5 and 7.

mental arrangement actually used, $\gamma = 39^{\circ}$, approximately, so $\sin \gamma \doteq 0.62$.

This series expansion for $\frac{W}{(\Delta\lambda_D)'}$ converges for all values of C, but of course no longer applies when C is so large that the contribution of the natural broadening process to the line shape must be taken into account. Other broadening processes can certainly be neglected.

In the usual theory which describes the formation of absorption lines by a gas where the atoms are in thermal equilibrium the same result is obtained without the factor $(\sin \gamma)$. The approximation involved in considering only doppler broadening is supposed to hold so long as C is less than about 5, although Hill[19] remarks that it may hold for C as large as 10. At any rate we shall be dealing only with lines for which C is less than 5, so we shall neglect natural broadening completely and assume that $\underline{a}$ is vanishingly small.

If the lines exhibit hyperfine splittings greater than the doppler width Eq. (2.18) is to be applied to each component separately. An example of this is given in the discussion of the absolute f-value determination for copper.

A check on the various numerical factors in Eq. (2.18) is possible if we consider the case of a very weak line. For C very small, Eq. (2.18) reduces to

$$\frac{W}{\Delta\lambda_D} = \sqrt{\pi} \sin \gamma \, C = \frac{\pi k_o K f}{2z_o} \sin \gamma. \qquad (2.19)$$

Replacing k_o by its value $\frac{\sqrt{\pi}\, e^2}{mc\Delta\nu_D} = \frac{\sqrt{\pi}\, e^2\lambda^2}{mc^2\Delta\lambda_D}$, we have

$$W = \frac{\pi^{3/2} e^2 \lambda^2 \, K \, f \sin \gamma}{2mc^2 z}. \tag{2.20}$$

The case of a very weak absorption line can also be readily calculated from the first principles. From Eq. (2.16)

$$W = \int_0^\infty \frac{I_\lambda(-x_o) - I_\lambda(x_o)}{I_\lambda(-x_o)} \, d\lambda = \frac{\lambda^2}{c} \int_0^\infty \frac{I_\nu(-x_o) - I_\nu(x_o)}{I_\nu(-x_o)} \, d\nu. \tag{2.21}$$

Eq. (2.11) gives, for a weak absorption line,

$$I_\nu(x_o) = I_\nu(-x_o) \left[1 - \int_{-x_o}^{x_o} N(x) \alpha_\nu(x) dx \right], \tag{2.22}$$

so Eq. (2.21) becomes

$$W = \frac{\lambda^2}{c} \int_0^\infty \int_{-x_o}^{x_o} N(x) \alpha_\nu(x) dx d\nu. \tag{2.23}$$

The integral over ν can be performed at once, using Eq. (2.3), so

$$W = \frac{\lambda^2 \pi e^2 f}{mc^2} \int_{-x_o}^{x_o} N(x) dx. \tag{2.24}$$

Substituting the value of N(x) given by Eq. (2.5), we have

$$W = \frac{\lambda^2 \pi e^2 f}{mc^2} K \frac{\sqrt{\pi}}{4} z \int_{-x_o}^{x_o} \frac{dx}{(z^2 + x^2)^{3/2}}$$

$$= \frac{\lambda^2 \pi e^2 f}{mc^2} K \frac{\sqrt{\pi}}{2z} \left(\frac{x^2}{z^2 + x^2} \right)^{1/2}. \tag{2.25}$$

Therefore

$$W = \frac{\pi^{3/2}\, e^2\, \lambda^2\, K\, f\, \sin\gamma}{2\, m\, c^2\, z} \quad , \tag{2.26}$$

which is identical with the result obtained in Eq. (2.20).

In order to determine K the rate is measured at which the atoms in the beam deposit on a small flat surface area located above the source and normal to the axis of the beam. The number per second in speed range v to v + dv which enter solid angle $d\Omega$ is given by Eq. (2.4a). Therefore the number which deposit on the differential area $d\xi\, d\eta$ on the plane z = b is given by

$$K \frac{\cos^2\theta}{r^2} \beta^2\, v^3\, e^{-\beta^2 v^2}\, d\xi\, d\eta \tag{2.27}$$

Here r is the distance from the source to the element of area. The total number per second which deposit on the area $d\xi\, d\eta$ is

$$\int_0^\infty K \frac{\cos^2\theta}{r^2} \beta^3\, v^3\, e^{-\beta^2 v^2}\, dv\; d\xi\, d\eta = \frac{K}{2\beta} \frac{\cos^2\theta}{r^2}\, d\xi\, d\eta = dG'$$

$$G' = \frac{K}{2\beta}\, b^2 \int \frac{d\xi\, d\eta}{(b^2 + \xi^2 + \eta^2)^2} \tag{2.28}$$

Note that G' is the total depositing rate in atoms per second and the integration extends over the area of the deposit.

For the case where the deposit is on a circular area of radius ρ located directly over the source,

$$\int \frac{d\xi\, d\eta}{(b^2 + \xi^2 + \eta^2)^2} = 2\pi \int_0^\rho \frac{\rho_1\, d\rho_1}{(b^2 + \rho_1^2)^2} \tag{2.29}$$

Therefore in this case

$$K = \frac{2}{\pi} G' \left(\frac{\rho^2}{\rho^2 + b^2} \right)^{-1} \sqrt{\frac{M}{2RT}} \quad . \tag{2.30}$$

It has been tacitly assumed in the derivation above that each atom included in N, which is determined by measuring the depositing rate, is capable of absorbing the line in question. At the relatively low temperatures (2000° K, or less) which are used to produce the atomic beam, this assumption is adequate if the ground state is single and lies well below other levels in the atom. Then all but a negligible fraction of the atoms in the beam will be in the ground state. This is the case, for example, for chromium, whose ground state is the single term $^7S_3$ which is 7593 cm^{-1} below the next lowest lying energy level. However, for iron the ground state is a ^5D term which is composed of five low lying levels, $^5D_{4,3,2,1,0}$, with a total spread in energy of only 978 cm^{-1}. In this case the Boltzmann distribution of the atoms among these states must be taken into account.

If, in a gas in thermodynamic equilibrium, there are N_o atoms in the lowest energy state, there will be

$$N_i = N_o \frac{g_i}{g_o} \exp\left(-\frac{E_i}{kT}\right) \tag{2.31}$$

atoms in the i -th state, where $g_i = 2J_i + 1$ and E_i is the energy of the i -th state. When the atoms in the beam deposit on a plane area and K is evaluated by measurement of the depositing rate, this measurement actually gives N_T, the total number of atoms in all energy states, where

$$N_T = \sum N_i = (N_o/g_o) \sum_i g_i \exp(-E_i/kT) \tag{2.32}$$

Therefore,

$$N_o = g_o N_T \left[\sum g_i \exp(-E_i/kT) \right]^{-1} \tag{2.33}$$

For Fe the sum need only be extended over the levels of the ^5D term since the population of the next higher term, a^5F, at 6928 cm^{-1}, will be negligible at the temperatures used.

After N_o has been evaluated Eq. (2.31) permits N_i to be determined for any other state. So G' can be suitably corrected to allow for the Boltzmann distribution of the atoms among the various low lying states.

C. Outline of Procedure for f-value Calculations

Having established the necessary theoretical relationships, we are now in a position to outline the procedure used in determining f-values from the measured equivalent widths of lines absorbed by the atomic beam.

A. The following quantities are measured:

(1) The temperature, T°K.

(2) The equivalent width, W in Angstrom units.

(3) The depositing rate, G in micrograms per second.

(4) The various dimensions:

ρ, the radius of the deposit

b, the height of the deposit above the source

γ, the half-angle of the atomic beam

z, the height of the light beam above the source

B. The following quantities are then calculated:

(1) The effective doppler width,

$$(\Delta\lambda_D)' = \sin\gamma \frac{\lambda_o}{c}\sqrt{\frac{2RT}{M}} = 4.30 \times 10^{-4}\,\lambda_o\sqrt{\frac{T}{M}}\,\sin\gamma,$$

where λ_o is in units of 10^{-5}cm. This then gives $(\Delta\lambda_D)'$ in Angstrom units.

(2)

$$\frac{2z_o}{\sqrt{\pi}\,k_o\,K} = \frac{2Rmc}{e^2}\;\frac{1}{\lambda_o}\;\frac{1.66 \times 10^{-18}M}{M}\;\frac{\rho^2 z}{\rho^2 + b^2}\;\frac{T}{G} = Q\,\frac{T}{G}$$

where $Q = 3.28 \times 10^{-3}\;\dfrac{\rho^2 z}{\lambda_o(\rho^2 + b^2)}$

The factor $1.66 \times 10^{-18}M$ converts G to G' in atoms per second.

C. The f-value is then calculated as follows:

$\frac{W}{(\Delta\lambda_D)'}$ is calculated and C is determined from the so-called curve of growth relation (Eq. (2.18)) taking into account hyperfine structure if necessary. Finally, $f = Q \frac{T}{G} C$ where G has been corrected for the Boltzmann distribution if the ground state is not simple.

It may be desirable here to indicate the physical significance of the quantities defined above. In the usual theory, as given by Mitchell and Zemansky, for example, $C = k_o N f \ell$, where ℓ is the length of the absorbing column. $(k_o N \ell)$ may be thought of as a measure of the effective number of absorbing atoms. In our theory $C = (G/QT) f$, so (G/QT) gives the effective number of absorbing atoms in this case.

D. Graphical Method for f-value Calculations

The method given in the last section for calculating f-values from the measured equivalent widths of the absorption lines depends for its validity on an accurate knowledge of the motions of the atoms in the atomic beam. If the assumption of molecular effusive flow is justified, then the theory as developed should be adequate. However, if the true flow pattern is significantly different from molecular effusion, a systematic error may appear in the calculated f-values. For this reason it is desirable to have at hand a method for calculating the f-values which is independent of the exact assumptions made regarding the motions of the atoms in the atomic beam. Such a method will now be described.

The specific assumptions which have been made about the atomic beam give rise to the factor $\sin\gamma$ in the final curve of growth relation, Eq. (2.18). This factor according to the theory is calculated from the geometry of the atomic beam (γ is half the angle subtended by the beam); then in Eq. (2.18), $(\Delta\lambda_D)' = \Delta\lambda_D \sin\gamma$. In order to achieve some independence from the exact assumptions involved in Eq. (2.18) let us postulate that the theory as developed gives the proper <u>form</u> for the curve of growth relation, but due to features of the atomic beam which have been ignored $\sin\gamma$ is to be replaced by μ, a parameter which depends upon the beam geometry in an unknown way. We will therefore write $(\Delta\lambda_D)' = \mu\Delta\lambda_D$ in Eq. (2.18).

Since the relationship between $\frac{W}{\Delta\lambda_D}$ and C is nonlinear for large values of the variables, the factor μ should be uniquely determinable from the experimental data. Indeed, it should be possible to determine both f and μ from the measured values of $W/\Delta\lambda_D$ and G/QT.

$$\log W/(\Delta\lambda_D)' = \log (W/\Delta\lambda_D) - \log \mu \qquad (2.32)$$

and, using the results of Section II-B,

$$\log C = \log \frac{G}{QT} + \log f. \qquad (2.33)$$

Therefore, the following procedure may be used for the reduction of the experimental data:

(1) On a sheet of graph paper plot the equation

$$\log (W/\Delta\lambda_D) = \log \sqrt{\pi} + \log C + \log \sum_{n=1}^{\infty} - (-1)^n \frac{C^{n-1}}{n! \sqrt{n}}. \qquad (2.34)$$

using $\log (W/\Delta\lambda_D)$ as ordinate and $\log C$ as abscissa. This will be called the "ordinary curve of growth."

(2) Plot the experimentally determined values of $\log (W/\Delta\lambda_D)$ vs the corresponding experimentally determined values of $\log (G/QT)$.

(3) Determine "by eye" how much the ordinary curve of growth must be shifted in both abscissa and ordinate so that it best fits the experimental points.

(4) Then the shift in ordinate gives $\log \mu$ and the shift in abscissa gives $\log f$ in accordance with Eqs. (2.32, 2.33)

The essential requirement for the above procedure to be effective is that the experimental values fall on the non-linear "knee" of the curve of growth. Clearly, if the experimental values define a linear curve, no unique assignment of μ and f is possible. The optimum method of conducting the atomic beam experiment depends, therefore, upon whether μ is equal to $\sin \gamma$. If this is the case, there are advantages to operating

in such a manner that the observed lines fall on the linear part of the curve of growth, since the f-values then suffer least from random errors in equivalent width measurement. On the other hand, if it should prove desirable to use the graphical method described above, it would be necessary to include lines well up on the knee of the curve.

The data obtained in the present experiment were reduced using both procedures. It was expected a priori that μ found by the procedure described above would agree with sin γ. However, in cases where sufficient data were available to estimate experimental curves of growth, μ appeared to be a factor of 1.4 - 1.6 smaller than sin γ. The resulting f-values were about twice as large as those calculated using the theoretical method.

The real origin of the discrepancy between μ obtained by the graphical method and sin γ determined by the geometry of the atomic beam is unknown at this time. It is presumed to arise from some property of the atomic beam which has not been adequately taken into account in the theoretical development. Further research, perhaps with a number of different beam geometries, in which both very weak and very strong lines are studied, may well solve the problem satisfactorily and put the final results on a firm basis.

E. Appendix: Momentum Transfer

When the shutter is opened and the atomic beam allowed to deposit on the balance pan, the pan experiences a force due to the momentum transfer from the atomic beam. We shall now calculate this force. Equation (2.27) gives for the mass deposited per second on an element of area $d\xi\, d\eta$, if M_o is the mass of one atom,

$$M_o d\xi\, d\eta\, K \frac{\cos^2\theta}{r^2}\ \beta^3 v^3 e^{-\beta^2 v^2}\ dv.$$

for atoms whose speeds are in the range v to v + dv. The force $d\dot{p}$ on area $d\xi\, d\eta$ is given by this expression multiplied by the normal component of velocity, v cos θ:

$$d\dot{p} = M_o d\xi\, d\eta\, K \frac{\cos^3\theta}{r^2}\, \beta^3 (v^4 e^{-\beta^2 v^2})\, dv. \qquad (2.35)$$

The total force is therefore

$$F = \dot{p} = \int d\dot{p} = M_o K \left(\frac{3}{8}\beta^2\sqrt{\pi}\right)\ 2\pi \int_o^\rho \frac{\rho b^3 d\rho}{(b^2+\rho^2)^{5/2}}$$

$$F = \frac{3}{8\beta^2}\pi^{3/2} M_o K \left(\frac{\rho^2}{b^2}\right), \qquad (2.36)$$

where terms $\mathcal{O}\left(\frac{\rho^4}{b^4}\right)$ are neglected, provided no reflection occurs. If reflection or re-emission of atoms from the balance pan occurs, $\dot{p}$ observed will be systematically larger than the value calculated using Eq. (2.36).

From Eq. (2.30)

$$K = \frac{2G\beta}{\pi}\left(\frac{b^2}{\rho^2}\right)$$

So

$$\dot{p} = \frac{3\sqrt{\pi}}{4\beta} GM. \qquad (2.37)$$

For small extensions the helix obeys Hooke's law so the force is related to the extension it produces by the equation $F = -kz$. Since the spring constant k for the helix is known, the force due to the momentum transfer can be measured by observing the extension it produces which is the "kick" mentioned in Section II-A(4). Table I shows the results for a particular run using iron where the measured forces are compared with the forces calculated using Eq. (2.37).

TABLE I

Run	$\dot{p}$ Calculated	$\dot{p}$ Observed	($\times 10^{-5}$ dynes)
1	65	35	
2	81	100	
3	150	160	
4	115	80	

Since there is no apparent tendency for the observed force to be greater than the calculated force, it was concluded that no significant fraction of the atoms was reflected. It is difficult to put a limit on the fraction which might be reflected on the basis of this experiment; Kopfermann and Wessel[17] performed an experiment to attempt to detect reflected atoms directly and concluded that for iron less than 3 percent of atoms were reflected or re-emitted.

III. DESCRIPTION OF THE APPARATUS AND EXPERIMENTAL METHODS

A. Atomic Beam Apparatus

1. Vacuum Chamber

The main vacuum chamber, the hood, was a large brass cylinder 8-1/2 in. in diameter and 10 in. high. Two quartz windows through which the light beam passed were sealed to side arms. One of these can be seen in the photograph, Fig. 10. The photomultiplier assembly used to monitor the temperature of the furnace, the bleeder valve, and the Pirani gauge were mounted on front and back ports. The photograph shows the photomultiplier assembly mounted on the front port. A few turns of 3/8 in. copper tubing soldered to the hood permitted cooling water to circulate.

The hood rested on a 1/2 in. thick brass plate which was mounted on adjustable legs. The electrodes and water lines to the interior of the apparatus passed through O-ring seals in this plate. Another brass plate formed the lid for the vacuum chamber. The rotating window assembly used for temperature measurements and the glass case which contained the quartz helix were mounted on this plate.

The hood was evacuated through a 1-1/2 in. manifold connected to the base plate. A sylphon bellows was installed in the manifold below the base plate to allow for small adjustments and leveling. Below the bellows was a 2 in. vacuum valve from which the manifold extended to a liquid nitrogen cold trap and to the diffusion pump. A DPI diffusion pump type VMF-100, rated at 100 liters per minute pumping speed, was used; it was backed by a Welch Duo-Seal forepump.

Figure 10 is a photograph of the apparatus as a whole. The pumps and

cold trap do not show since they are behind and below the main vacuum chamber.

All demountable seals were made using O-rings, with the retaining grooves cut in accordance with the manufacturer's specifications. They were found to give completely satisfactory service. Although the system had to be brought up to atmospheric pressure after each run and a number of the O-ring seals taken apart, ordinarily little trouble was encountered in reassembling the apparatus and in pumping down again. The ultimate vacuum usually obtained after pumping overnight was $2\text{-}3 \times 10^{-5}$ mm-Hg.

The pressure was measured by means of an RCA 1949 ionization gauge tube in conjunction with a power supply and vacuum tube voltmeter circuit. A Pirani type gauge was also installed and was used as a rough vacuum gauge for leak checking.

The system was brought up to atmospheric pressure after a "run" by bleeding in helium from a high pressure tank through the bleeder valve. When the quartz helix was used it was found necessary to bleed in helium very slowly in order to prevent large oscillations of the helix. For this purpose the bleeder valve was fitted with a small bore capillary and an auxiliary throttling valve.

When the system was originally assembled most of it was painted with Glyptal Red Enamel, not only to localize remaining leaks, but also as a procedure to eliminate the possibility of leaks due to porosity in the large brass pieces. Screw holes and any long channels which might have constituted virtual leaks were either relieved or provided with pump-out holes.

2. Furnace

The requirements for a satisfactory furnace to produce the atomic beam

were as follows:

(1) Temperatures up to about 2000°C would be required. The temperature should be readily controllable and relatively insensitive to fluctuations in line voltage.

(2) The actual source of the atomic beam should be of small area.

(3) The angular spread of the beam should be kept as large as possible so that the geometrical factor sin γ would be close to unity.

(4) It should be possible to change operation readily from one element to another.

The furnace finally adopted made use of a thin wall graphite tube mounted horizontally at right angles to the direction of the light beam as the heating element. A "boat" of graphite which fit loosely in the furnace tube contained the material to be evaporated; the actual source of the atomic beam was a hole in this boat. Figure 3 shows the tube and boat assembly.

The furnace tube was 0.375 in. in diameter and 2-1/2 in. long with a wall thickness of 0.023 in. It was made by drilling out a 2-1/2 in. length of spectroscopic graphite rod according to the following procedure. The rod was mounted in a collet in a metal working lathe, one end was faced off and center drilled. The rod was then drilled approximately half way through with a 1/4 in. straight-flute drill. It was removed from the collet, turned around, and the same procedure repeated. Then several progressively larger drills were used without turning the rod again until the inside diameter was 21/64 in. This procedure made the machining of the furnace tubes

relatively easy and minimized the risk of breaking the graphite during the machining operation. After drilling out the rod to the required inside diameter a 1/4 in. hole was drilled in its wall at the midpoint. This hole was enlarged by filing until it was roughly elliptical in shape, 1/4 in. wide and about 1/2 in. long.

The tube was heated by passing a current of up to 300 amperes through it from a step-down transformer. The transformer was rated at 200 amperes/11 volts continuous service. It could, however, be operated at current loads as high as 300 amperes for brief periods of time with no signs of undue heating. The current leads between the transformer and the furnace were of 3/8 in. copper tubing through which water circulated. The primary voltage was supplied from a 40 ampere Variac connected to the 115 volt line.

The material to be evaporated was placed in a "boat" of graphite located at the center of the furnace tube. The boat was fabricated from a 7/8 in. length of 3/8 in. graphite rod turned to the proper shape and bored out to a 3/16 in. inside diameter. The open end was then closed off with a plug of graphite. A hole was drilled in the wall of the boat to be the source of the atomic beam. For most of the runs the diameter of this hole was 0.070 in. The last runs for each of the elements studied, however, were made using boats with 0.150 in. holes. This dimension is so large that the hole is no longer an orifice; the free surface of the evaporating metal is the real source. The shape of the boat was roughly like a spool. The ends were machined to fit snugly in the furnace tube, then were filed so that contact was left in only three places at each end to center the boat in the furnace tube. This procedure insured that the electrical contact

between the boat and the tube would be poor so that the boat would not short out the furnace tube.

In operation the boat was located in the tube so that its orifice was in the center of the hole in the wall of the tube. The tube and boat were shaped so that the atoms leaving the orifice in the boat would not strike any other part of the boat or the tube.

The heating of the boat was by radiation from the furnace tube. Since the tube surrounded most of the boat its temperature was usually only 30 to 40 degrees Centigrade lower than the temperature of the tube. The ultimate temperature which could be reached depended upon a number of factors, particularly upon the amount of "shorting out" of the furnace tube by the boat. Temperatures in excess of 1700°C could always be attained if reasonable care were exercised in making the boats. For higher temperatures it was necessary to use a radiation shield around part of the tube. This shield was formed from 0.005 in. molybdenum sheet and when in place permitted operation at temperatures higher than 2000°C.

The ends of the graphite furnace tube were fitted smugly into short copper cylinders which were clamped to massive copper blocks. These blocks were mounted on the ends of brass rods which served as current leads. They were water cooled by means of an internal double channel; they were insulated from the base plate by means of O-rings which also provided the necessary vacuum seals.

3. Water Jacket and Defining Slot

A water jacket surrounded the graphite tube assembly. This jacket was constructed of copper and had a system of internal channels through which water circulated. It formed an integral part of the slot assembly which

served to define the angular spread of the atomic beam.

The slot in the water jacket was 1/2 in. wide and 0.750 in. long. It was located approximately 0.450 in. above the orifice in the boat. (This distance was accurately measured before a run to determine the half-angle of the beam.)

Directly over the furnace assembly a copper plate was mounted which served to define the portion of the beam which was collected for the depositing rate measurement. This plate was mounted on four legs which were attached to the top surface of the water jacket assembly; its height was adjustable by the use of spacers. Water cooling for the upper plate was provided by an internal channel which was fed through two glass tubes connecting to the water jacket assembly. The upper plate was designed so that it could be electrically insulated from the rest of the apparatus if this ever should prove to be desirable. It was provided with seven 3/8 in. holes over which sheets of mica or aluminum were placed for the depositing rate measurements prior to the acquisition of the quartz helix. When the furnace was assembled the orifice in the boat was centered by sighting through the center hole in the upper plate. Then, with the boat satisfactorily centered, the positions of the holes in the upper plate were accurately known relative to it.

After installation of the quartz helix all the holes in the upper plate were covered over except the center hole and one close to the end of the plate. The center hole was used to define the fraction of the atomic beam which would strike the balance pan; the temperature of the interior of the boat was measured by observing it with an optical pyrometer through the hole in the end of the plate as will be described in a later section.

A vane of 0.010 in. molybdenum sheet was mounted below the upper plate on a shaft which could be rotated from outside the vacuum system. This vane served as a shutter to shield the upper plate from the atomic beam except during an actual run.

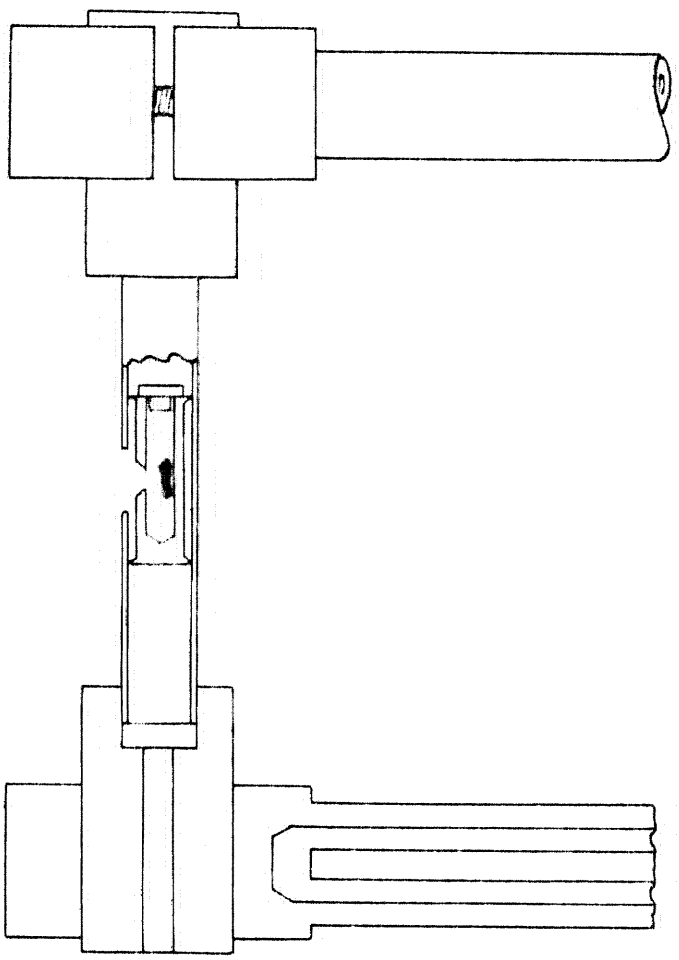

FIG. 3 FURNACE ASSEMBLY

B. Temperature Measurement and Control

1. Method of Temperature Measurement

The temperature of the atoms in the atomic beam was measured by means of an optical pyrometer which "looked" directly at the evaporating metal in the boat. The temperature actually used in the calculations was the color temperature of the inside of the graphite boat. Both the copper and chromium melting points were observed in this way and found to agree with the accepted values to within 10°C.

The evaporated metal, of course, deposited on any window through which a direct observation of the inside of the graphite boat might be made. In order to circumvent this difficulty a disk of glass was installed in the line of sight which could be rotated from outside the vacuum system to provide a fresh window each time the temperature was measured.

The entire optical system between the source and the optical pyrometer was calibrated to correct for the effects of absorption in the glass and reflections at the various surfaces. The calibration was made by determining experimentally the temperature vs current curve for a tungsten ribbon filament lamp, first with all the various optical elements in the light path, then with the pyrometer alone. The difference between these curves on the temperature axis gave the correction to be applied to the observed color temperatures to give true color temperatures. The curves so obtained had a good deal of scatter, but a sufficient number of points were determined to enable the temperature correction to be known within about 10°C, which is better than one percent at the temperatures used. A straight line was drawn through the experimental points and the following relation obtained for use between observed temperatures 1000°C to 2000°C:

$$T = 1.084\ T_{obs} + 328. \qquad (3.1)$$

In this relation T_{obs} is the observed temperature in ^{o}C and T is the corrected temperature in ^{o}K.

The above equation gives the correction for the rotating window, the window in the vacuum chamber, a 90^{o} prism which was used so that the pyrometer could be operated in a horizontal position, and a lens which magnified the image of the boat so as to facilitate the temperature measurement. It was necessary to adjust the optical elements so that a minimum of light was reflected or scattered into the pyrometer. If it proved to be impossible to make the pyrometer filament disappear even though it seemed to be the same color as the interior of the boat, the presence of reflected or scattered light was indicated and the optical system was realigned.

2. Temperature Regulation

Precise control of the temperature of the furnace emitting the atomic beam is a much more critical problem than is measurement of the absolute value of the temperature. This is because the rate of evaporation or vapor pressure of metals varies markedly with temperature. The relationship between vapor pressure and temperature is usually given in the form

$$\ell n\ P = -\frac{A}{T} + B. \qquad (3.2)$$

For a metal such as iron, A is very large -- of the order of 50,000. (See Kelley[13].)

To get an idea of the precision of temperature control required, let us consider a case where A = 50,000 and T = 1500°K.

Then

$$\frac{\delta P}{P} \doteq 33 \frac{\delta T}{T} . \qquad (3.3)$$

So, if the evaporation rate is to be held constant to within 10 percent the absolute temperature must be held constant to within 0.3 percent, or about 4°K. This may be taken as the maximum allowable temperature variation.

The temperature was stabilized by means of an electronic regulator circuit. A 931A photomultiplier was mounted on a side tube attached to the hood so as to receive radiation from the graphite boat. (See the photograph, Fig. 10) The photomultiplier current should be roughly proportional to the total radiation from the boat. Since the boat is essentially a black body, its total radiation will be proportional to T^4 (Stephan-Boltzmann Law). Therefore, a 0.3 percent change in temperature will result in about a one percent change in photomultiplier current. Since the total current was about 20 microamperes, such a change would be 0.2 microamperes. The photomultiplier was operated at a fixed voltage of 67.5 volts per dynode. An iris diaphragm permitted adjustment of the amount of radiation received by the photomultiplier so that at a particular furnace temperature the photomultiplier current could be set at about 20 microamperes.

Figure 4 shows the circuit of the temperature regulator. A battery operated voltage pentode was used as the photomultiplier anode load impedance. The effective load impedance was in excess of 20 megohms although

the voltage drop across the pentode was only about 20 volts. Thus a relatively large signal appeared on the grid of the amplifier pentode. This signal was amplified and provided the driving voltage for the control circuit. Control of the furnace current was achieved through two 6AS7 twin triodes connected in parallel across the primary of the low-voltage transformer whose secondary was in the circuit of the transformer which provided the furnace power. The impedance of the 6AS7's is reflected into the primary circuit and so, if their parallel impedance changes, this change results in a change in the mean voltage drop across the low-voltage transformer secondary. The entire grid swing of the 6AS7's gave a range in voltage drop across the secondary of the low voltage transformer from 3 to 8 volts when 20 amperes flowed in this circuit.

When the control circuit is connected into the main transformer circuit and the photomultiplier tube receives radiation from the graphite boat, and when the various voltages are adjusted so that the tubes are in the operating ranges, the circuit constitutes a closed feedback loop. It was found that for line voltage variations of 5 volts the temperature was held constant to better than 0.1 percent.

The actual operation of the control circuit is as follows: The filaments are allowed to warm up for 10 - 15 minutes prior to operation. The furnace is brought up to approximately the temperature desired. Then the iris is opened until the photomultiplier current is approximately 20 microamps. P-1 and P-2 are now adjusted until the circuit is operating. A simple way of verifying that the controller is working is to change the main Variac voltage slightly and observe whether the

controller compensates for the change. It is well to check that the amplifier tube grid is not drawing excessive current by noting if any appreciable change in the anode current results from closing the shorting switch. Any large voltage fluctuations must be compensated manually with the main Variac.

The circuit described above was entirely successful in maintaining the temperature constant to better than the required precision.* As a check on the constancy of the evaporation rate two exposures were usually taken at each temperature setting. The equivalent widths of the absorption lines obtained from these two exposures checked within the accuracy with which they could be measured except for several cases when the evaporating metal was apparently exhausted before the second exposure had been completed.

It was found that if the furnace was run late in the evening when there were no large fluctuating loads on the line the temperature often stayed constant within the desired limits without regulation. It was necessary to use the regulator during the day, however, since large line voltage fluctuations often occurred then. The temperature would be monitored by shorting out the control circuit and substituting a galvanometer for meter M_1. When this was done a bucking current was used to zero the galvanometer at any desired photomultiplier current.

---

*With the circuit values given in the Parts List, p. 43, the lowest temperature which could be controlled was about 1200°C. Suitable modification should allow operation down to about 1000°C with photomultiplier currents as low as 2 μamps. These modifications would include changing the value of B_4 and probably substituting a 1U4 or similar tube for the 3Q4 (V_3).

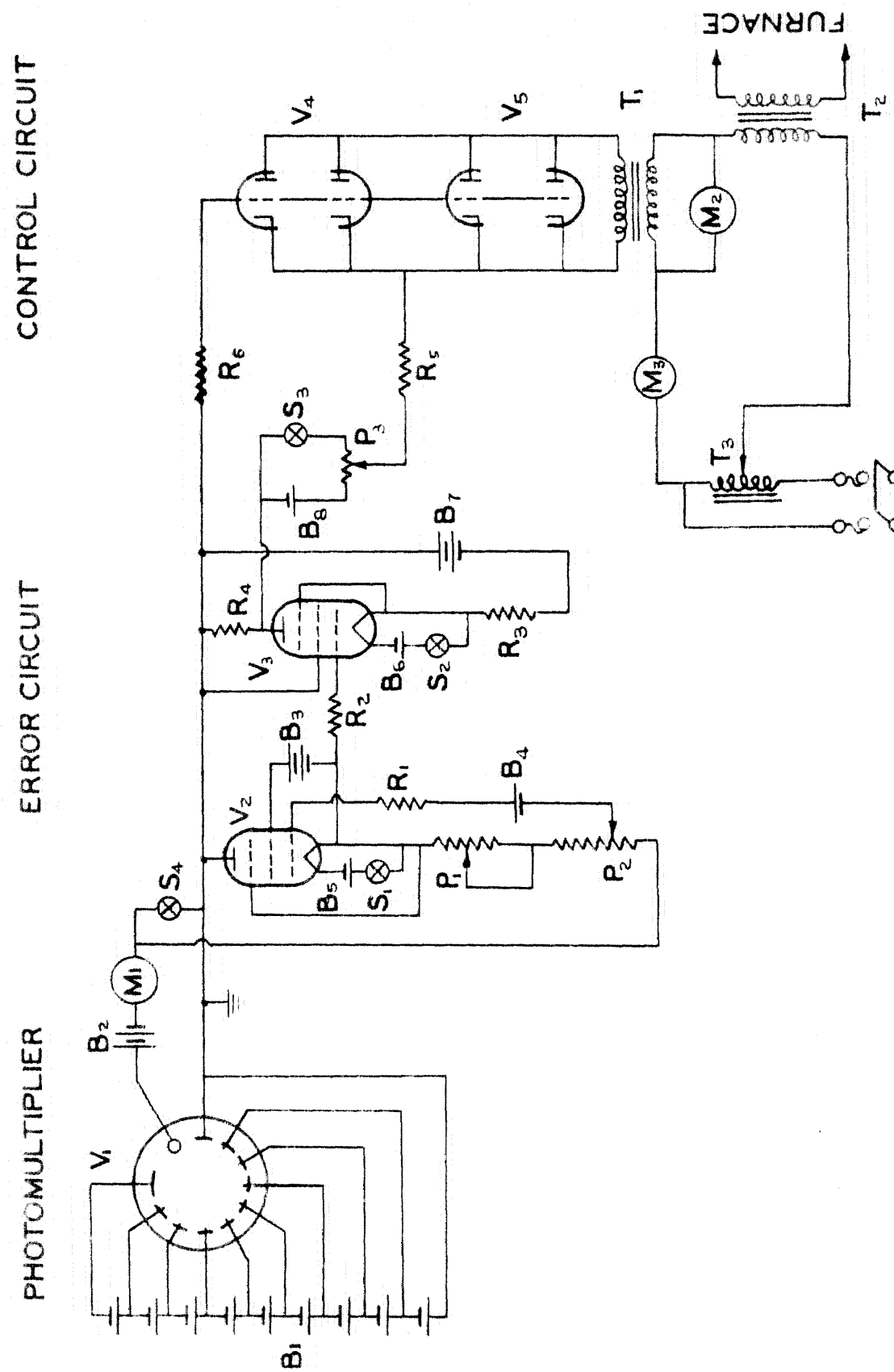

FIG. 4 TEMPERATURE CONTROL CIRCUIT

PARTS LIST

Batteries

B_1	Battery pack, 67.5 volt "B" batteries to supply dynodes.
B_2	2 67.5 volt "B" batteries in series
B_3	67.5 volt "B" battery
B_4	22.5 volt "A" or "B" battery, with taps every 1-1/2 volt
B_5, B_6	1.5 volt "A" batteries
B_7	90 volt "B" battery
B_8	45 volt "B" battery

Tubes

V_1	931-A photomultiplier
V_2	1U4 miniature pentode
V_3	3Q4 miniature pentode
V_4, V_5	6AS7 twin triodes

Resistors

R_1	2.2 megohms
R_2	390 K ohms
R_3	220 ohms
R_4, R_5, R_6	22 K ohms

Transformers

T_1	110 v - 5 v Kenyon
T_2	110 v - 12 v 200 amp Westinghouse
T_3	Variac 40 amp

Potentiometers

P_1	1.5 megohms
P_2	3 megohms
P_3	100 K ohms

Meters

M_1	0-50 μamp dc
M_2	0-8 volts ac
M_3	0-50 amp ac

Switches

S_1, S_2	SPST ganged together
S_3	SPST
S_4	SPST shorting switch

C. Depositing Rate Determination

1. Mica and Aluminum Sheets

The method fordetermining the depositing rate which was used throughout the first stage of the experimental work made use of light sheets of mica about 1 cm square. Prior to a run these sheets were carefully cleaned and weighed to the nearest microgram. They were then placed over the holes in the upper plate. While an exposure was being made the shutter was opened for a measured length of time, then the sheets were removed from the vacuum and weighed again to determine the weights of the deposits. The weights of the evaporated metal films were usually between 20 and 100 micrograms. From the position of the sheets relative to the source, the weights of the deposits, and the time for which the shutter had been open, the depositing rate was calculated as described in the section on theory.

It was soon found that the depositing rates calculated from the weights of the several sheets on which the atomic beam deposited during a single run varied as much as 20 percent among themselves. A number of procedures were tried to remedy this situation:

(1) A high voltage lead was installed in the top of the vacuum chamber and the sheets were subjected to a high voltage gas discharge prior to a run; it has been found that such a discharge has a cleansing action. It was hoped that the deposit would stick better to the sheets if they were cleaned in this way.

(2) The mica was split very thin so that the total weight of each sheet was of the order of 10 milligrams. This was done in an effort to increase the accuracy of weighing.

(3) Special precautions were taken to insure that there would be no absorption of water vapor by the deposited film.

None of these measures made any difference in the observed scatter in rates of deposit. Glass cover glasses and sheets of 0.0008 in. aluminum sheet were tried on the theory that the scatter might be due either to moisture trapped in the mica or to flaking of the mica during handling. No improvement was noticed with either glass or aluminum, although aluminum was finally adopted since the aluminum sheets were easier to handle than were the mica sheets.

Although the scatter in rates of deposit persisted no systematic difference with respect to position of the sheets in the beam was observed to indicate that the predicted beam distribution was in error. It was found that if the rates obtained from three or more sheets from a single run were averaged the results usually were consistent from one run to the next. No satisfactory explanation for the observed scatter has been suggested.

2. Quartz Helix

The method of measuring the rate of deposit of the atomic beam described in the preceding section had, in addition to unexplained random inherent errors, the possibility of including systematic errors due to oxidation of the deposit or absorption of water vapor prior to final weighing. To avoid these possibilities and as a check on the results, a quartz helix was installed inside the vacuum system to measure the rate of deposit by weighing in vacuo. The helix was suspended in a glass case mounted directly over the furnace. (See photograph, Fig.10.) A pan was made from a 3/4 in disk of 0.0008 in.

aluminum foil to which a hook of No. 38 Nichrome wire was fastened with a speck of Duco cement. The edges of the pan were crimped to prevent buckling. During a run the pan was suspended about one centimeter above the central hole in the upper plate. The pan was made considerably larger than the hole to insure that all of the beam passing through the hole would be caught even if the pan were slightly off center.

The quartz helix was purchased from Microchemical Specialties, Berkeley, California. It had the following dimensions:

Diameter of fiber	0.094 mm
Diameter of helix	2 cm
Number of turns	67
Length unloaded	24 cm

To calibrate the helix two standard weights of No. 38 Nichrome wire were made. The linear density of the wire was accurately determined from the weight of a 90 cm length, then two short pieces were cut and their lengths accurately measured. The weights were calculated and then were checked by direct weighing. The linear density obtained for No. 38 Nichrome was 0.6715 mg/cm and the two standard weights were:

No. 1 0.997 mg

No. 2 0.550 mg.

The balance pan weighed about 12 mg. It was hooked onto the fiber, and the extensions produced by the two weights were measured. By this means there was no difficulty in establishing the calibration to better than one percent. At a total extension of about 12 cm, the sensitivity was 1.00 cm/mg, which corresponds to a spring constant of 0.98 dynes/cm.

The extension of the helix was read by means of a vertically mounted microscope which was fitted with a micrometer eyepiece. Large differences were read on the traveling microscope; the smallest division was 0.001 cm and there was no difficulty in estimating to 0.0001 cm. For small differences a more convenient procedure was to use the micrometer eyepiece since it was more easily adjusted without jarring the table and hence disturbing the helix equilibrium. One division on the micrometer eyepiece corresponded to 0.000237 cm.

When mounted in a vacuum the helix tended to rotate as a unit and the cross fiber provided by the manufacturer was very difficult to focus on. It was found to be most convenient to set the cross hairs of the micrometer eyepiece on a small spherical knob in the fiber.

To increase the visibility of the fiber it was illuminated from the side by means of a microscope illuminator. A horizontal band of light then appeared across the center of the spherical knob on which settings were easily made even when the helix was rotating.

In air small oscillations of the helix, which have a period of about one second, were damped out in several seconds. However, in a vacuum chamber very little damping occurs at pressures less than 10^{-4} mm-Hg. Because of this it was usually necessary to take the mean of the limits of the oscillation as the point of equilibrium unless it was convenient to wait until the oscillation had finally damped out. (This usually took 5 - 10 minutes.) It would be advantageous to attach a light vane of metal to the helix so that a magnet outside the balance-case could be used to damp out the oscillations by means of eddy currents.

During a run the balance was used as follows: The equilibrium position

of the fiber was noted. Upon opening the shutter the first "kick" of the helix was noted. This kick is due to the momentum transfer from the atomic beam to the balance pan as discussed in Section II-E. Then, after a measured period of the time (1 - 3 minutes), the shutter was closed and the new equilibrium position was read. From the calibration factor for the helix the extension due to the weight of the deposit on this pan was converted to micrograms. Because of the possibility of temperature changes affecting the equilibrium position the reading after a run was made as soon as possible.

The helix proved to be remarkably rugged and no special precautions were needed in its handling. When pumping down the system with the helix in position the pumping speed was sufficiently slow at the start so that no special precautions had to be taken to protect the helix. However, in bringing the system up to atmospheric pressure it was necessary to be careful to bleed in helium very slowly in order not to jar the helix by a rush of gas. After the system was at atmospheric pressure the entire balance case together with the brass base to which it was attached was taken off the main vacuum chamber and set off to one side on a bench.

The results obtained using the quartz helix to measure the depositing rates checked well with the results obtained using the aluminum sheet rate determinations. This consistency was taken as an indication that there had been no systematic error using the aluminum sheets.

Perhaps the greatest advantage of the helix was that a number of "runs" at different depositing rates could be recorded in succession on a single photographic plate without bringing the system up to atmospheric pressure after each run as had previously been necessary when the aluminum sheets had to be removed and weighed to determine the depositing rate.

D. Optics

1. Light Source and Lens System

The light source used was a high pressure mercury arc lamp manufactured by the Huggins Laboratories of Menlo Park, California. This lamp operated at a power level of about 1 kilowatt and produced a very satisfactory "pseudo-continum" of pressure broadened mercury lines. It was found that for satisfactory operation of the lamp a voltage was needed somewhat in excess of that obtained from the Philips "1000 volt" lamp transformer available in the laboratory. In order to provide a higher voltage the secondary of the Philips transformer was connected in series with the secondary of a G. E. H-6 lamp transformer. Both transformers have a strong ballast action and serve to limit the current which the lamp can draw to about one ampere. The G. E. H-6 transformer was operated with a Variac in its primary circuit to allow for selection of the optimum operating voltage. It was found that when the lamp had run for a few hours it was necessary to raise progressively the primary voltage on the H-6 transformer from about 60 to about 100 volts to maintain satisfactory operation.

A considerable improvement resulted from a small modification in the lamp assembly. The ground connection in the lamp holder did not always afford a good electrical contact with the lamp. If this connection became uncertain, the voltage across the lamp dropped and its operation became unstable. In order to correct this defect a thin phosphor bronze strip was soldered to the ground terminal of the lamp. This strip then formed a dependable electrical connection with the brass fixture which formed the ground lead.

The lamp was water cooled. The use of tap water for this purpose had the disadvantage that after several months of use the interior of the quartz water jacket which surrounded the lamp would begin to become opaque from the mineral content of the water. This deposit was, however, readily cleaned out by a weak acid solution, and such a periodic cleaning seemed to give less trouble than a system for circulating distilled water which was tried for a time.

The mercury arc lamp was operated with the capillary in a horizontal position. A system of two quartz lenses formed a reduced image (about 1/3) of the lamp in the center of the atomic beam inside the vacuum envelope (see Fig. 1). The result of forming a horizontal image of the capillary in the center of the atomic beam was that the light beam effectively formed a very thin horizontal sheet which passed through the atomic beam at a well determined height above the source. The sheet of light was so thin (about 2 mm) that its extension in the z-direction could be neglected in the calculations. The beam was picked up and rendered parallel by a 60 cm quartz lens and a final image of the lamp was formed on the slit of the spectrograph by a second 60 cm quartz lens. The image of the lamp was parallel to the slit. All of the apertures were chosen so that the grating itself formed the limiting aperture for the system.

Since the extension of the image of the lamp in the y-direction (as well as in the z-direction) was small compared to the dimensions of the atomic beam, no correction for this extension was necessary. There was, therefore, no need to attempt to correct for losses of light in the spectrograph.

2. Spectrograph

The spectrograph used for this experiment was the 21 ft Rowland Spectrograph located in the Bridge Laboratory of the California Institute of Technology. The first order was always used; the inverse dispersion was 2.64 Angstrom units per millimeter. The vertical mounting of this instrument was particularly convenient since the pit, in which the grating and its supporting beams are mounted, is light-tight and during an exposure no particular care had to be taken to prevent fogging of the plate by lights in the room above. The pit also serves to keep the instrument at a constant temperature. The focus was checked periodically by photographing the spectrum of the iron arc using a medium contrast emulsion as described by Hill[19]. It was rarely necessary to make any adjustment in the slit height.

The slit width customarily used was about 0.03 mm. In order to be sure that no error resulted from the use of such a comparatively wide slit, the absorption spectrum of I_2 vapor was photographed using slit width of 0.03 mm, and again using a narrow slit width of 0.005 mm. When microphotometer tracings were made of these two spectra no differences in line shapes were observed. It was therefore concluded that the experimental results were not dependent upon slit width, at least for widths in this range.

A test was made to determine the amount of light scattered by the spectrograph. It was found that when a Kodak Wrattan 2-B filter which cuts off light to the violet of 4000 A was used the intensity of the Hg-arc observed in the ultraviolet for wavelengths shorter than 3900 A was diminished by a factor greater than 50. This means that less than

2 percent of the observed intensity at 3700 A, say, resulted from scattering from longer wavelengths. It is more difficult to determine whether scattering from shorter wavelengths might occur, but there is no reason to expect that it would be important.

E. Photographic Plates

1. Choice of Plates

The ideal photographic plate for this experiment would have had a relatively fast emulsion with both a very high contrast and negligible grain size. Unfortunately no such emulsion exists. Two emulsions were used in the course of the experimental work, Cramer Contrast and Kodak Fine Grain Positive. The Cramer plates are faster and have a somewhat greater contrast than the Kodak Fine Grain Positive plates but they have a considerably larger grain size. It was felt that the very fine grain structure of the Kodak FGP emulsion outweighed the disadvantage of relatively low contrast and so the Kodak plates were used for most of the last runs. The difference in speed was about a factor of three which was not enough to be a serious disadvantage. The exposure times used for the Kodak FGP plates were usually of the order of one minute. On the linear part of the characteristic curve (%-blackening vs log of light intensity), for the spectral region around 3700 A, a one percent change in blackening corresponded to a change of about 0.0054 in log intensity for the Cramer Contrast plates, and to about 0.0075 for the Kodak FGP plates. For wavelengths near 3200 A the "calibration factor" increases to about 0.0120 for the Kodak FGP plates, which is rather large, but even here the very small grain size more than compensated for the relatively low contrast.

2. Development

The Cramer Contrast plates were developed for 4 minutes in D-19 developer at 20°C, the Kodak FGP plates were developed for 3 minutes in a-76 developer at 20°C. Brush development was used in an effort to minimize the Eberhard effect.

3. Calibration

The plates were calibrated by means of a step slit. A tungsten ribbon filament lamp was used as the light source. It was supplied from a low-voltage transformer which was operated from a Variac and a Sola constant voltage transformer. The filament was imaged on the step slit which had nine steps whose widths had been accurately measured. The lamp current was kept constant to one percent and a set of exposures were made on a plate which was developed along with the plate to be calibrated. (The procedure was essentially the same as described by Hill[19].)

Two step slits were used, one (No. 1) for high contrast plates, the other (No. 2) for plates of moderate contrast. For calibration of the Cramer Contrast plate, particularly, step slit No. 2 proved to be advantageous. The following table gives the width measurements of the step slits.

TABLE II

Step	Step Slit No. 1 Log Width	Step Slit No. 2 Log Width	
1	1.818	1.366	(Widths are measured in units of 0.1 mm.)
2	1.647	1.307	
3	1.468	1.261	
4	1.295	1.205	
5	1.129	1.161	
6	0.963	1.102	
7	0.805	1.050	
8	0.629	0.984	
9	0.478	0.915	

When the densities of the step slit spectra had been determined a graph of %-blackening vs log step-width was plotted. (The light intensity entering the spectrograph was proportional to the width of the slit since the image of the ribbon filament was wider than any step used.) With both the Kodak FGP and the Cramer Contrast plates the curve from 30 percent to 75 percent blackening was linear and its slope could be determined with considerable precision. This slope, expressed as the change in log-intensity corresponding to a change of one percent in blackening, was called the "plate calibration factor." Multiplication of the "depth" of the absorption lines as they appeared on the microphotometer tracings by this factor converted the depth to Δ(log-intensity).

F. Microphotometer

After a plate was exposed and calibrated as already described the strengths of the absorption lines were measured on the recording photoelectric microphotometer of the Mount Wilson Observatory. Again the procedure described by Hill[19] was followed in most particulars. The only modification in his procedure was the use of the various amplification factors now available on the microphotometer. It is possible after a line has been traced to go back over it with the galvanometer deflections amplified by a choice of factors between 1.4 and 20. Such amplification increases the precision with which very weak lines can be measured. It was always used in conjunction with at least one tracing of the line at unit amplification to be sure of the density of the continuum and to serve as a check. The linear magnification factor (X100) was used throughout, as in Hill's work.

Each line and the neighboring continuum was traced at least twice, usually three or four times, so that an average could be taken and some of the effects of grain noise thereby eliminated. The actual reduction of the data was made as follows:

(1) The plate calibration curve was drawn as already described and the calibration factor determined.

(2) The tracings of the lines were marked as described by Hill. The lines observed were always weak, by Hill's standards, so they were assumed to have a triangular shape. Triangles were drawn which best approximated the observed line shapes. The heights of the triangles in %-blackening were converted to Δ(log intensity) by multiplying by the calibration factor.

Since very few lines appeared on any plate it was nearly always possible to select a suitable exposure time such that the continuum would be in the proper density range for all lines.

The intensity of light in the continuum near the line was taken to be the intensity incident on the atomic beam. The equivalent widths were then found by approximating the integral,

$$W = \int_0^\infty \frac{I_o - I_\lambda}{I_o} \, d\lambda$$

by

$$W = \frac{I_o - I_{\lambda o}}{I_o} \quad \frac{BD}{2},$$

where $I_{\lambda o}$ is the intensity at the center of the line, B is the base width of the line in mm and D is the inverse dispersion of the spectrograph in A/mm. For a particular line the value of $(1 - I_{\lambda o}/I_o)$ was calculated from the value of $\Delta(\log I)$ and then multiplied by the base width and by 1.32 (which is one-half the inverse dispersion) to obtain the equivalent width.

IV. RESULTS AND CONCLUSIONS

In this section the absolute f-values which were obtained for the resonance lines of Cr I, Mn I, Fe I, and Cu I will be presented and discussed, along with resumes of previous work and details of any experimental techniques employed which were peculiar to a particular element. In most cases the results are preliminary in the sense that it is not possible to draw experimental curves of growth according to the procedure given in Section II-D which permit unequivocal determination of μ and f. For this reason the results of both the graphical method, using the values of μ and f which seemed to fit the data best; and the theoretical method are reported. The f-values found by these two procedures differ in most cases by a factor of about 2. Several arguments are presented in favor of the values obtained by the graphical method, but these admittedly are not conclusive. In most cases further data on very strong lines should resolve the difficulty; recommendations for further research are made in the various sections on the individual elements. The desirability of including measurements of very strong lines in the research program was not realized until all of the data reported in the present paper had been obtained.

---

*In the curve of growth relation for lines formed by an atomic beam $\Delta\lambda_D$ is replaced by $(\Delta\lambda_D)'$. The atomic beam theory presented in Section II-B gives $(\Delta\lambda_D)' = (\Delta\lambda_D) \sin\gamma$, where γ is half the angle subtended by the atomic beam. The "graphical method" given in Section II-D differs only in $(\Delta\lambda_D)' = (\Delta\lambda_D)\mu$, where μ is considered to be an unknown parameter and is determined from the experimental data.

It has been assumed in applying the graphical method that the failure of the experimental data to follow the predicted curves of growth is a real effect and is not due to a systematic error in the equivalent width measurements. A check on the validity of this assumption will come when strong lines have been measured in the Mn I spectrum. The Mn I lines should follow a linear curve of growth, so a systematic deviation from such a curve could be attributed to a systematic error in the measurements. The data on Mn I lines are insufficient at the present time to settle this point definitely, but the data which are available do not appear to indicate the presence of such a systematic error.

A. Chromium

Chromium is one of the more important elements of the iron group for which absolute f-values might be determined. This importance arises both from its intrinsic astrophysical interest and because a relatively large amount of information about its relative f-values is available from the work of Hill[19]. Although the absolute f-values of the Cr I resonance lines have been the subject of several investigations, at the present time there is some doubt even of their order of magnitude.

Estabrook[15, 16] determined the absolute f-values of the CrI resonance lines λλ 4290, 4275, and 4254 by the method of total absorption. The experimental technique he used was the same as that developed by King and Stockbarger[12]. A small amount of chromium metal was placed in a quartz cell which was evacuated, baked out, and sealed. The cell was heated under carefully controled conditions and the Cr I resonance lines were observed in absorption at a temperature of about 1150° C. Estabrook in his first paper[15] used the vapor pressure data given by Kelley[13] which were the best then available. In a later paper[16] he revised his results in the light of new data on chromium vapor pressure reported by Speiser, Johnston, and Blackburn[20]. Further vapor pressure measurements have recently been made by Gulbransen and Andrew[21]. Their results agree well with those of Speiser, Johnston and Blackburn, so Estabrook's revised f-values are probably fairly reliable.

Huldt and Lagerqvist [22] have recently measured the absolute f-values of chromium by an emission method. They sprayed a solution containing Cr O into a C_2H_2 - air flame. Then from the measured temperature of the flame (which they state may be unreliable), the calculated partial pressure of

Cr vapor in the flame, the dissociation energy of Cr O, and the absolute intensity of the Cr I lines, they calculated the absolute f-values. The values they obtained were smaller than those reported by Estabrook by a factor of about 100.

Although Estabrook's results seem more reliable than those of Huldt and Lagerqvist, his f-values certainly cannot be considered well established. It was decided, therefore, to redetermine the absolute f-values of the Cr I resonance lines by the atomic beam method. The physical properties of chromium are fairly typical of the metals in the iron group and for this reason it was used for most of the preliminary testing of the apparatus. It was felt, for instance, that if a furnace could be designed which would operate satisfactorily at the temperatures required to vaporize chromium (about 1600° C) and if an atomic beam could be formed, then the problem would essentially have been solved for all of the nearby elements as well. The only peculiarity exhibited by chromium was its disagreeable tendency to sputter while evaporating. This sputtering sometimes resulted in the orifice of the graphite boat becoming plugged with solid material; an occurrence which necessitated the replacement of the boat. When the quartz helix was used, on several occasions a small piece of chromium thrown off from the evaporating metal struck the balance pan causing the helix to oscillate wildly. The actual weight of such pieces was probably somewhat less than 0.1 microgram, so the depositing rate measurements were probably not disturbed appreciably by the sputtering. It is possible, however, that some of the scatter in the experimental points may be of this origin. The depositing rate measurements would also be rendered invalid if an appreciable change in weight due to oxidation

were to occur. Gulbransen and Andrew[21] carried out a detailed investigation of the oxidation of chromium films. On the basis of their work it is safe to assume that the gain in weight of a chromium film due to oxidation upon exposure to air will be very slight if the film is at room temperature, and that oxide formation in a vacuum will be completely negligible.

In the present experiment a number of plates were taken using chromium before the experimental procedure had been fully worked out. Some of the data from these early plates were subsequently discarded. Table III, page 64, gives the experimental results obtained from plates 001, 005, 017, 018, 019, and 020, which were taken using the "old method" of depositing rate determination (mica and aluminum sheets), and 043, for which the depositing rates were determined by the quartz helix. On plate 043 only the 4200 triplet was measured; on the other six plates all of the Cr I resonance lines, λλ4290, 4275, 4254; 3605, 3593, 3578 were measured. The table gives the absolute temperature used; the measured depositing rate, G, in micrograms per second; the quantity G/QT which is a measure of the effective number of absorbing atoms (see Section II-D); and the measured equivalent width divided by the doppler breadth, $W/\Delta\lambda_D$, for each of the lines. The f-values for the lines were calculated from these data using $(\Delta\lambda_D)' = \Delta\lambda_D \sin\gamma$ as given by the atomic beam theory and averaged. The results are tabulated in Table IV, page 65, under the heading "f-values (1)." The data were also plotted in order to apply the graphical method.

Figure 5a shows all the experimental points with a tentative curve of growth drawn through them. An "ordinary curve of growth" is also shown

for comparison. The points were plotted using the following procedure: (1) The data for λ3578, the strongest Cr I resonance line, were plotted. (2) The values of G/QT for the other lines were multiplied by the ratios of their f-values to f_{3578} (the calculated f-values were used to determine these ratios). Then the data for the other lines were plotted along with the data for λ3578.

There is so much scatter in the points that an experimental curve of growth cannot be readily drawn through them. In order to overcome this difficulty the log (G/QT) axis was divided into eleven sections, each 0.1 units wide, which included all the experimental data. Then the values of log $(W/\Delta\lambda_D)$ in each section were averaged. These averages are plotted in Fig. 5b, where the vertical lines through each point give an estimate of the probable error of the average. The idea behind this procedure was that the scatter was primarily due to random errors in the equivalent width measurements which resulted from plate calibration errors, line marking errors, etc. If the scatter were really the result of errors in the depositing rate determinations, the procedure as described would not be valid. The solid line in Fig. 5b represents the curve of growth which seemed to be the best fit for the average points. This curve was shifted vertically by -0.36 units and horizontally by 0.71 units from the ordinary curve of growth, so $\mu = 0.43$ and $f_{3578} = 0.195$. The f-values which were obtained by the graphical method for λ3578 as described above, and for the other lines using their f-values relative to λ3578, are given in Table IV under the heading "f (2)."

The dashed line in Fig. 5b is the curve of growth which would be obtained if the f-value for λ3578 obtained by the other procedure (0.120) were used along with $\mu = \sin \gamma = 0.62$. It is apparent from the figure that the data on the Cr I lines are not sufficiently accurate, nor do they extend to strong enough lines, to allow a completely satisfactory conclusion to be drawn. The theoretical curve of growth is not excluded by the data.

In summary, the results of the present experiment definitely indicate that the f-values reported by Hult and Lagerqvist are in error by several orders of magnitude. The f-values found by the graphical method, though in fairly good agreement with Estabrook's revised values, may be revised considerably when more data become available. The scatter in the points was too great to allow for a reliable graphical determination of f_{3578}. The f-values calculated from the data on the basis of the atomic beam theory were lower than Estabrook's values by a factor of about 2.

TABLE III Cr I DATA

Plate	T °K	G	G/QT	$W/\Delta\lambda_D$ λ4254	$W/\Delta\lambda_D$ λ4275	$W/\Delta\lambda_D$ λ4290	G/QT	$W/\Delta\lambda_D$ λ3578	$W/\Delta\lambda_D$ λ3593	$W/\Delta\lambda_D$ λ3605
001	1873	0.222	13.3	0.505	0.421	0.385	11.2	0.940	0.851	0.618
005	1926	0.085	4.92	0.370	0.270	0.182	4.14	0.768	0.527	0.402
017	1935	0.163	9.21	0.508	0.363	0.254	7.75	0.840	0.685	0.564
018	1858	0.208	12.2	0.385	0.381	0.306	10.4	1.02	0.814	0.658
019	1903	0.132	7.60	0.388	0.311	0.256	6.40	0.830	0.800	0.728
020	1845	0.102	6.05	0.230	0.232	---	5.10	0.490	0.474	0.386
043 (1)	1703	0.035	2.44	0.124		---				
(2)	1703	0.035	2.44	0.105		---				
(3)	1736	0.057	3.96	0.198	0.110	---				
(4)	1736	0.057	3.96	0.170	0.193	---				
(5)	1779	0.081	5.46	0.324	0.280	0.130				
(6)	1779	0.081	5.46	0.400	0.240	0.158				
(7)	1811	0.123	8.20	0.358	0.324	0.176				
(8)	1817	0.099	6.60	0.321	0.250	0.195				
(9)	1817	0.099	6.60	0.340	0.260	0.130				
(10)	1865	0.134	8.60	0.391	0.280	0.213				

TABLE IV

Cr I Absolute f-Values

Transition		Wavelength	f(Estabrook)	f(H and L)	f(1)	f(2)
$a^7S - z^7P^o$	3-2	4289.72	0.047	0.00055	0.025	0.041
	3-3	4274.80	0.067	0.00076	0.031	0.050
	3-4	4254.35	0.084	0.00097	0.048	0.078
$a^7S - y^7P^o$	3-2	3605.33		0.0016	0.076	0.123
	3-3	3593.49		0.0022	0.098	0.159
	3-4	3578.69		0.0028	0.120	0.195

In the above table Estabrook's values are those from his revised paper, Ref. 16, the values in the column headed "H and L" are those reported by Hult and Lagerqvist[22]. The results of the present experiment are given in columns (1), and (2). The values in column (1) were calculated using the atomic beam theory, those in (2) were estimated by the graphical method.

The factor by which Hill's relative f-values are to be multiplied to obtain absolute f-values is 3.1×10^{-4} from the results of column (1), and 4.7×10^{-4} from the results of column (2).

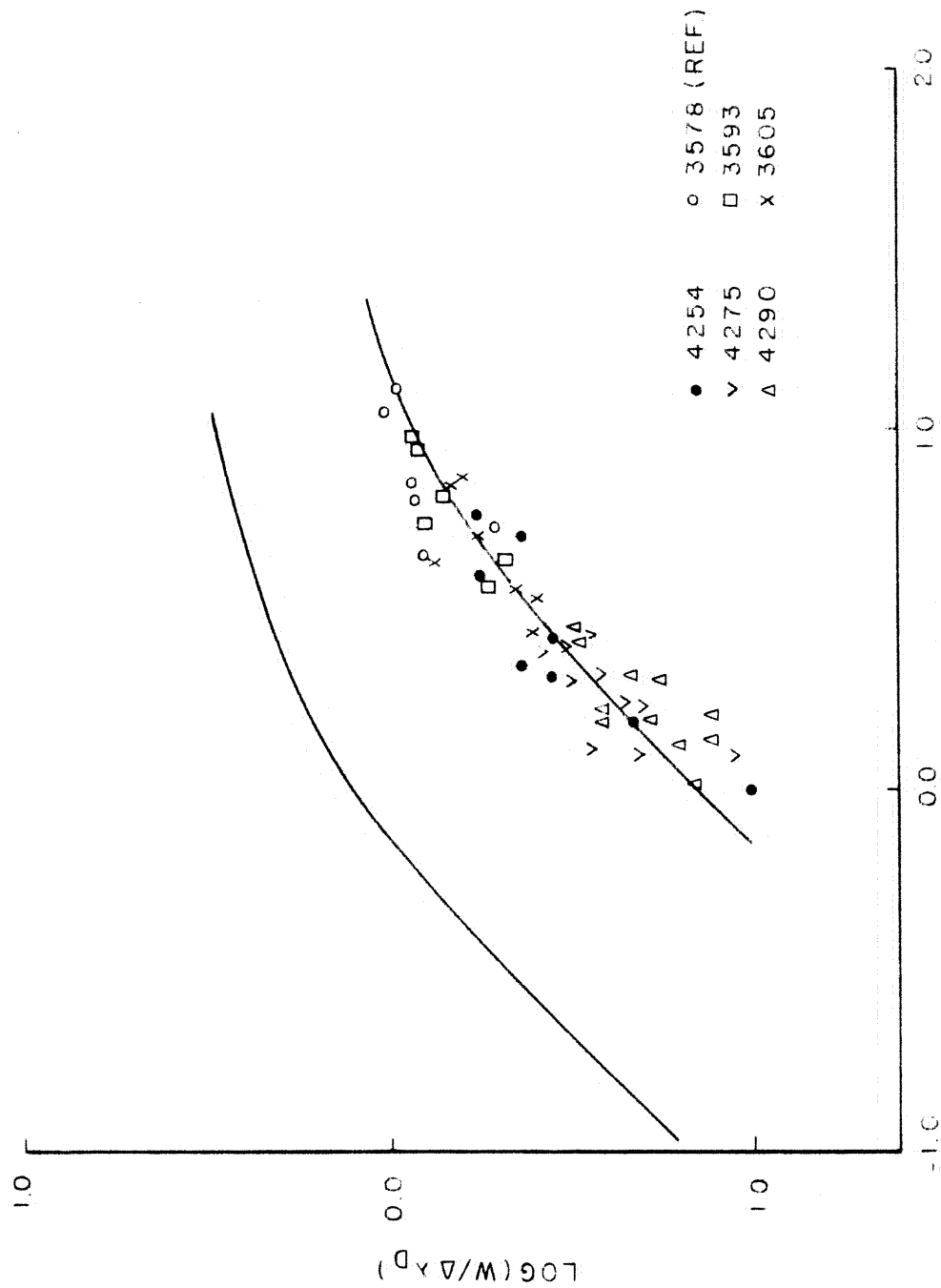

FIG.5a CHROMIUM

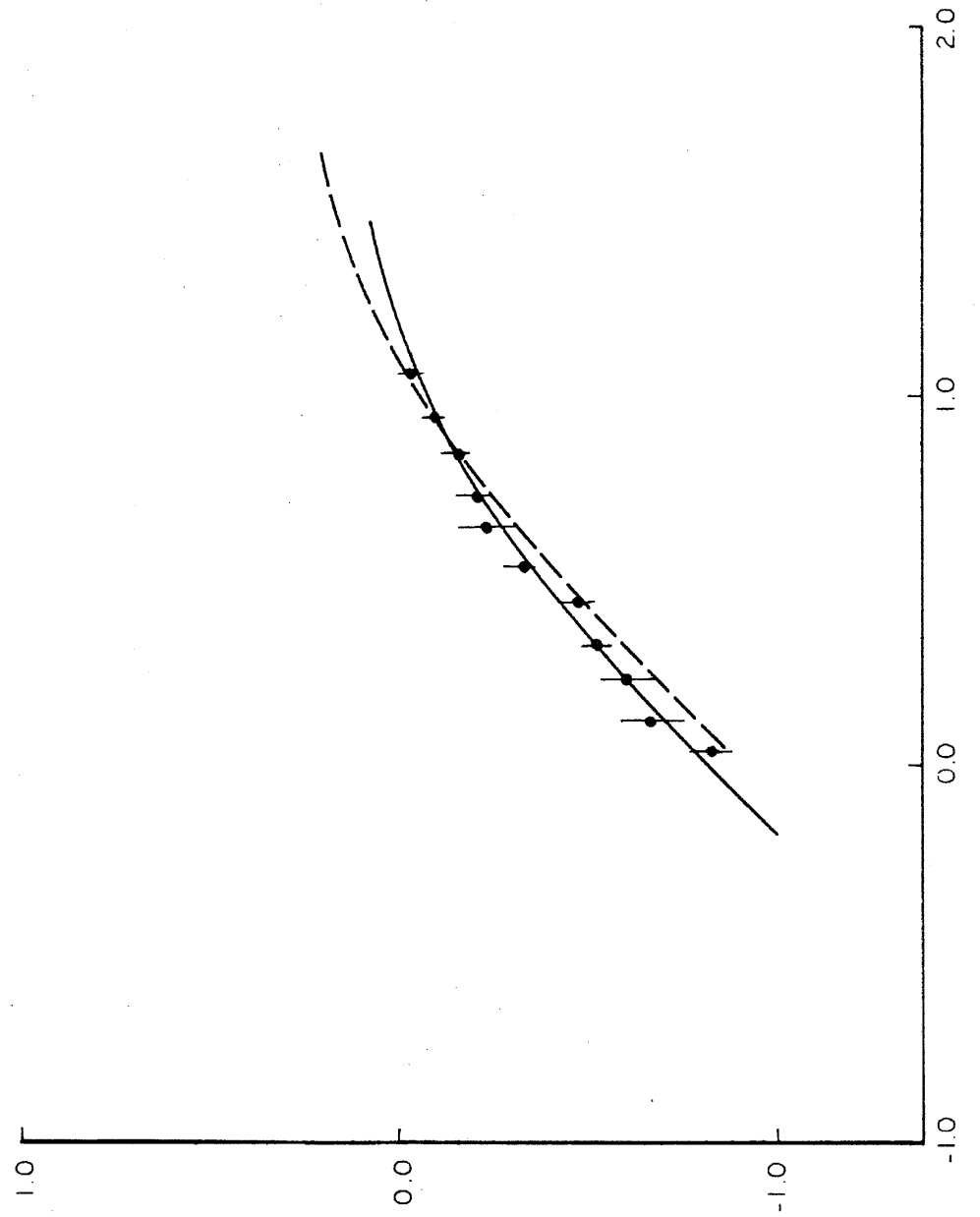

FIG. 5 b

B. Manganese

Very little is known about the f-values of the Mn I lines at the present time. A program to determine relative f-values for this spectrum will probably be carried out under Dr. Robert B. King within the next several years, but even when the results of this research are available, it may be difficult to establish absolute f-values for the lines. The ground state of manganese is separated by 2.11 ev from the first excited state. The only lines in the visible or near ultraviolet regions which arise from the ground state are λλ 4030, 4033, and 4034. Some preliminary work on the relative f-values for the spectrum using the King furnace indicates that other lines will be observed only under conditions where the 4000 triplet is too strong for the f-values to be calculable using the theory of total absorption. This means that it may prove to be very difficult to relate the f-values of the 4000 triplet to those of the rest of the lines. However, work is in progress on methods for overcoming this obstacle, and so it may be possible eventually to establish absolute f-values for the Mn I lines of interest. There is, of course, value in having absolute f-values available for the three resonance lines, whether or not the remainder of the spectrum can be satisfactorily related to these.

The only previous work on the Mn I resonance lines was done by Huldt and Lagerqvist[22] using a procedure similar to that already described in the section on chromium. Although their absolute f-values for Cr I are undoubtedly in error, the values which they obtained for Mn I are in rough agreement with the preliminary results obtained in the present experiment.

Up to the present time only one plate has been taken using manganese, so only preliminary results can be given. Judging from past experience, however, unless a large and unexpected calibration error occurred, the results should not drastically change when more data are available. The data were processed in a manner somewhat different from that used for the other spectra studied. Manganese has a nuclear spin of 5/2 and a relatively large magnetic moment. Since its ground state is an S state, it can be anticipated that its resonance lines will exhibit large hyperfine structure splittings. (See Mack[23].) The observed Mn I lines are therefore expected to follow a linear curve of growth. This means that the graphical method cannot be applied; μ and f cannot be determined independently from the data. On the basis of the experimental results to date, f-values were calculated using the first (linear) term of the power series in C.

The data for Mn are given in Table VI along with the calculated f-values. These data are plotted in Fig. 6 in the manner described previously. λ4031 was used as the reference line in Fig. 6. The f-values for $\lambda\lambda$4031, 4033, and 4034 are given in Table V.

Hult and Lagerqvist quote a probable error of 50 percent in their results, so the agreement between the preliminary f-values obtained in this experiment and their reported f-values may be satisfactory.

TABLE V. Mn I ABSOLUTE f-VALUES (PRELIMINARY)

Transition		λ	f (H and L)	f
$a^6S - z^6P^o$	5/2 - 7/2	4030.75	0.062	0.027
	5/2 - 5/2	4033.07	0.046	0.019
	5/2 - 3/2	4034.49	0.031	0.014

TABLE VI. Mn I DATA

	$T^{\circ}K$	G	G/QT	$W/\Delta\lambda_D$ $\lambda 4031$	f_{4031}	$W/\Delta\lambda_D$ $\lambda 4033$	f_{4033}	$W/\Delta\lambda_D$ $\lambda 4034$	f_{4034}
(1)	1401	0.0314	2.54	0.250	0.089	---	---	---	---
(2)	1449	0.128	10.0	0.420	0.038	0.291	0.026	0.191	0.017
(3)	1483	0.266	20.5	0.545	0.024	0.411	0.018	0.292	0.013
(4)	1542	0.738	53.0	1.35	0.023	1.08	0.018	0.678	0.011
(5)	1439	0.138	10.8	0.288	0.024	0.167	0.024	---	---

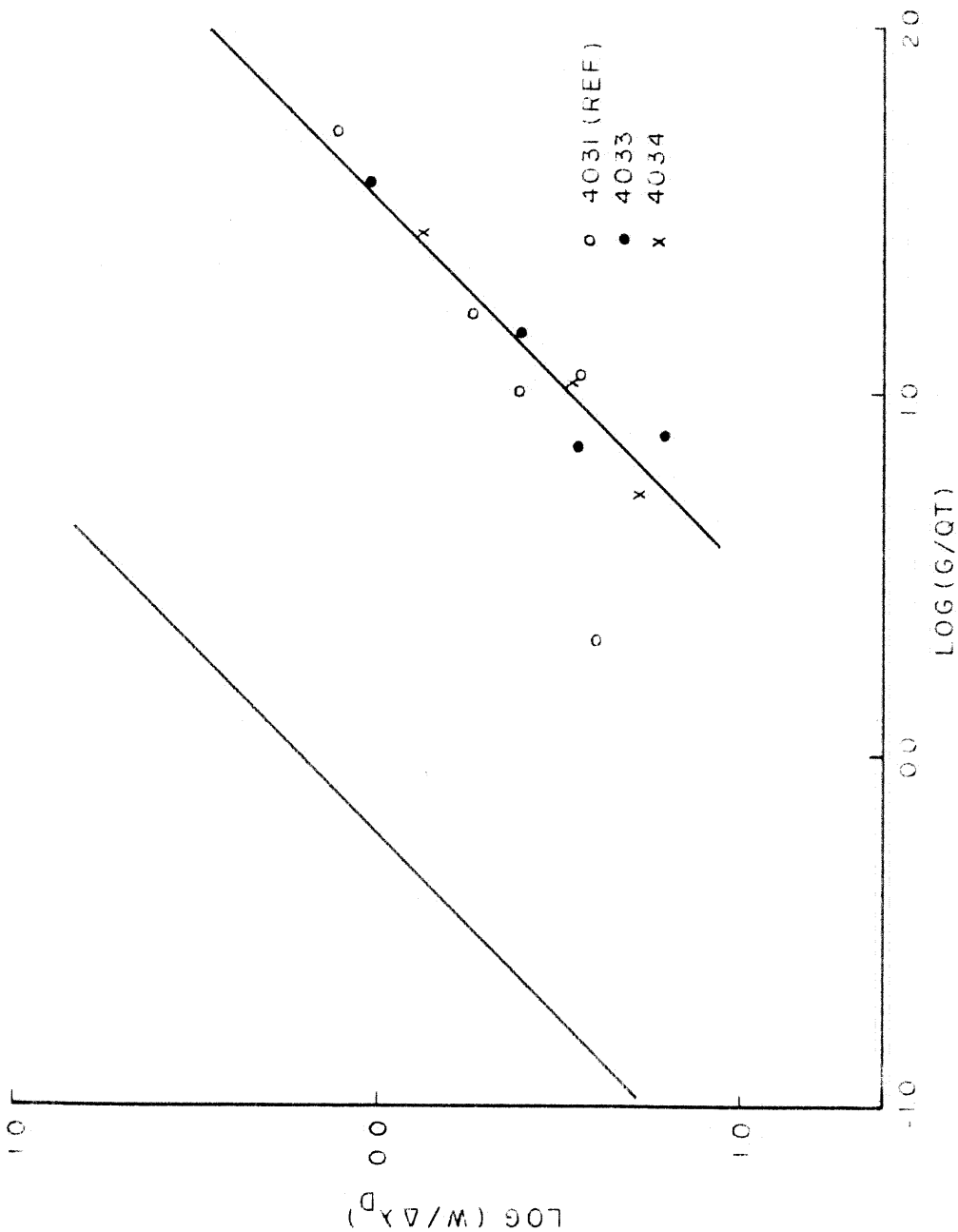

FIG. 6 MANGANESE

C. Iron

Iron is an element of great astrophysical interest. It is relatively abundant in stellar objects and its spectrum is rich in lines in every useable wavelength region. The relative f-values of many of the Fe I lines are known from the work of King and King[11] and Carter[24]. This work is at the present time being extended to include lines from high levels. The absolute f-values for lines in the Fe I spectrum were measured by King[14] by the method of total absorption. He used spectroscopically pure iron, a small sample of which was placed in an evacuated quartz absorption cell. The cell was heated in an electric furnace with particular care taken that the temperature was uniform. In order to compute the number of absorbing atoms he used the vapor pressure data of Marshall, Dornte, and Norton[25]. In his paper the f-values for twelve lines from the ground state are reported; the f-value for λ3719, the strongest of these, is given as 0.0130.

Kopfermann and Wessel[17] subsequently measured the f-values of λ3719 by an atomic beam method similar to the one used in the experiment reported here. The principal differences between their experiment and the present one were in the light source they used and in their method of measuring the strength of the absorption lines. Their light source was a hollow cathode which produced the iron resonance lines unreversed and with pure doppler contours. A photocell was used rather than a photographic plate to measure the absorption which took place when the light passed through the atomic beam. This turned out to be a particularly sensitive method of measuring the strength of absorption lines. The f-value they obtained for λ3719 was 0.043 ± 0.0008, a factor of 3 larger than the value reported by King.

As already stated, one of the original motivations for the present experiment was to redetermine the absolute f-value of the Fe I lines so as to resolve the difference between the results of Kopfermann and Wessel, and those of King. Chromium was studied first, however, because iron presented certain experimental difficulties. It was found that when a graphite boat was used no appreciable evaporation occurred until temperatures in excess of 1900°C were reached. This difficulty was noted by Kopfermann and Wessel; it is due to the solubility of carbon in molten iron. A satisfactory solution to the difficulty was achieved by lining the boat with a layer of TaC.

The procedure used to line the boat with TaC was as follows: The boat was made in the usual manner. Then a liner of 0.005 in. tantalum sheet was made; two disks for ends and a rectangle which was formed into a cylinder for the center section. The liner was slipped into the boat which was then "fired" in the electric furnace at the Mount Wilson Laboratory at a temperature of about 2600°C. This firing operation in the presence of an abundance of carbon converted the tantalum completely to TaC. With boats lined with TaC no difficulty was experienced in evaporating the iron at temperatures in the range 1700° - 1800°C.

Another difficulty arose from the fact that the Fe I f-values are small; and, moreover, at the temperatures used only about half the atoms are in the lowest state, a^5D_4. The remainder are distributed in accordance with the Boltzmann distribution over the other low states, $a^5D_{3,2,1,0}$. The result of these two factors is that even the absorption lines from the lowest state were too weak to measure reliably unless relatively

large beam densities were used. The order of magnitude of $N\ell$, the number of atoms per unit volume times the length of the absorbing column, was $1 \times 10^{12} cm^{-2}$ which is a factor of 10 larger than in the experiment of Kopfermann and Wessel. Operating with such a large $N\ell$ may be undesirable, since the larger this quantity is, the greater is the possibility that the atomic beam distribution may not correspond with the predicted distribution.

Seven plates were taken using iron, the data from all seven were used. Plates 029, 030, 031, 032, 035, and 036 were all taken using the "old method" of depositing rate determination; the quartz helix was employed for plates 040 and 041. As in the case of chromium the data obtained when the quartz helix was used showed no systematic differences from the data for which mica and aluminum sheets had been used. All of the plates provided useable data for λ3719, the strongest line from the lowest atomic state, a^5D_4. The observed values of $W/\Delta\lambda D$ and $G/\mathfrak{T}$ for λ3719 are tabulated in Table VIII, page 77.

Other lines were observed on some of the plates, in particular λλ3737, 3745, 3748, and 3860. The first three of these arise from the higher sublevels of the ground state; the fourth, λ3860 arises from the lowest state, a^5D_4. It is a member of the transition array $a^5D - z^5D^o$, while the other lines mentioned, along with λ3719, belong to the transition array $a^5D - z^5F^o$. Although the f-value of λ3737 is known from both the work of King, and of Kopfermann and Wessel, to be approximately equal to that of λ3719, its observed intensity was lower by a factor of about 2. This is because the energy of the state from which it arises, a^5D_3, is

0.05 ev above a^5D_4 and so a smaller fraction of the atoms in the atomic beam are in this state and can absorb the line. The same consideration applies to λλ3745 and 3748, which arise from states 0.09 and 0.11 ev above the lowest state, respectively. Since these lines were only observed on certain plates and their f-values relative to f_{3719} were accurately known from the work of King, it was decided to concentrate on measurements of λ3719 in the present experiment. λ3860, which also arises from the lowest state, was usually observed, but the exposure of the continuum near this line was too light to permit an accurate measurement of its equivalent width if the exposure was correct for λ3719.

Figure 7 shows the data for λ3719 plotted as described in Section II-D. The data were best fitted by a curve of growth with $\mu = 0.38$, $f = 0.048$. This curve is shown as a solid line; the dashed line is the curve of growth for $\mu = 0.62$, and $f = 0.022$, as calculated from the theory. The experimental curve seems to fit the points better than the theoretical curve, but data will have to be obtained on stronger lines before a definite conclusion can be made. When f-values were calculated using the theoretical method, taking $(\Delta\lambda_D)' = \Delta\lambda_D \sin\gamma$, a systematic tendency for the larger equivalent widths to yield smaller f-values was noticed. It was this tendency in the case of λ3719 which suggested that the data might not be following the predicted curve of growth and which led to the development of the graphical method given in Section II-D. The calculated f-values are included in Table VIII to illustrate this trend.

Table VII shows the f-values for λ3719 of the Fe I spectrum which

have been obtained to date. The column headed "f (1)" gives the result of the theoretical calculation; the column headed "f (2)" gives the result of the graphical method, with $\mu = 0.38$. The results of King[14] and Kopfermann and Wessel[17] are also given for comparison. The absolute f-value obtained in the present experiment is larger than King's result by either method of calculation; the graphical method gives good agreement with Kopfermann and Wessel. It will be important to extend these measurements to include stronger lines, so that a definite assignment of the absolute f-value of λ3719 can be made.

TABLE VII. Fe I ABSOLUTE f-VALUES

Transition	λ	f(King[14])	f(K and W[17])	f(1)	f(2)
$a^5D - z^5F^\circ$ 4-5	3719.93	0.013	0.043	0.022	0.048

TABLE VIII. Fe I DATA

Plate	T°K	G	G/QT	$W/\Delta\lambda_D$ λ3719	f(Calculated)
029	2086	0.715	33.1	0.423	0.028
030	2160	1.53	69.4	0.575	0.019
031	2200	0.580	25.4	0.352	0.030
032	2167	1.19	64.0	0.515	0.018
035	2189	2.28	121.0	0.895	0.020
036	2205	2.51	141.0	0.900	0.014
040 (2)	1828	0.093	5.25	0.164	0.062
(3)	1843	0.171	9.60	0.222	0.048
(4)	1880	0.325	17.9	0.191	0.022
(5)	1903	0.133	7.24	0.107	0.028
(6)	1958	0.096	5.40	0.096	0.035
041 (3)	2033	0.791	40.3	0.536	0.027
(5)	2040	0.652	31.2	0.364	0.026
(6)	2109	0.992	48.5	0.425	0.020
				Average	0.022

The data for 040 were not included in the average f (calculated). The very large f-values obtained for spectra (2) and (3) on this plate are probably the result of errors in equivalent width measurement. Rather than arbitrarily exclude these spectra, however, it was felt that a more consistent procedure would be to eliminate the plate entirely from the average. If these data are included, the average becomes 0.028.

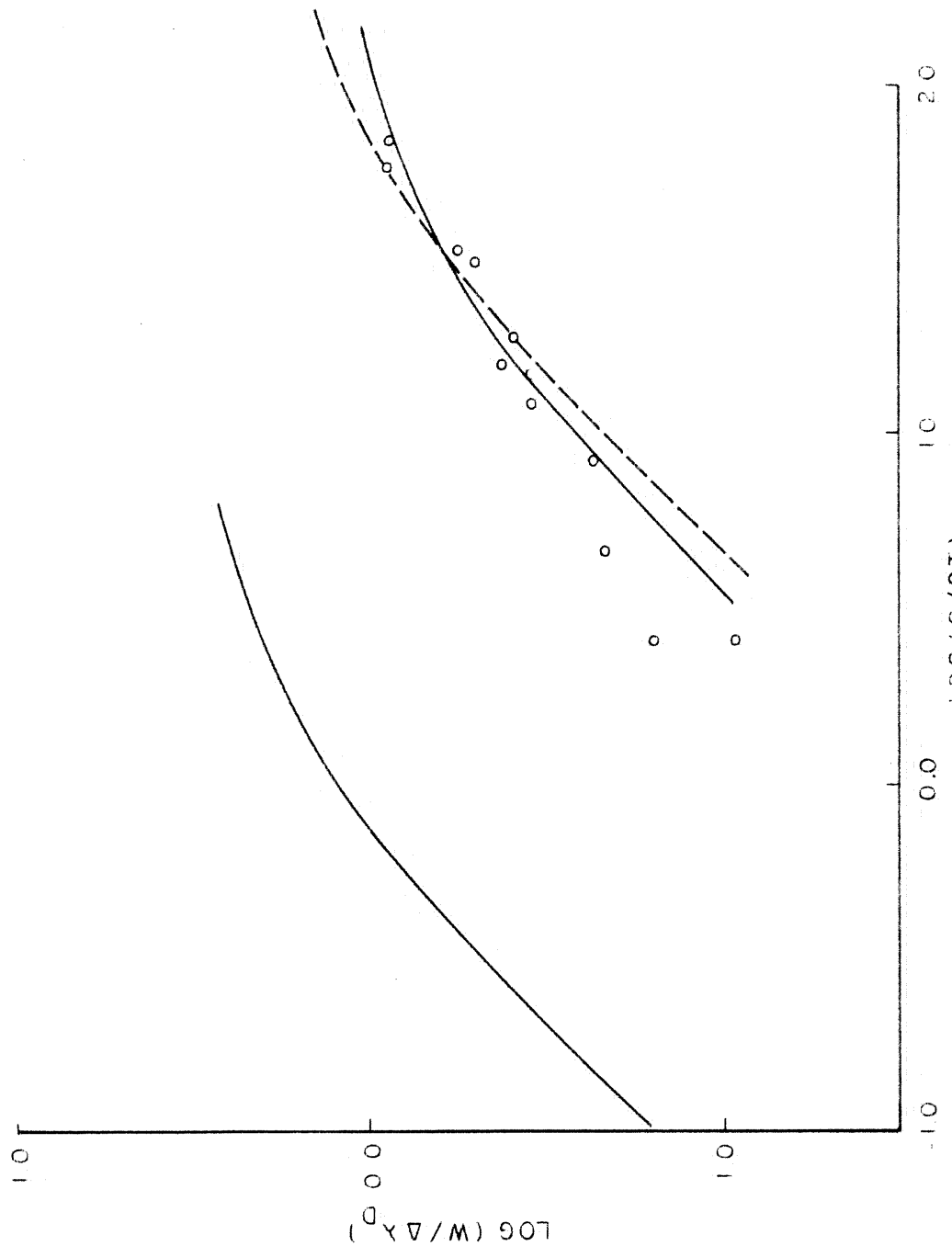

FIG.7 IRON λ 3719

D. Copper

The Cu I spectrum is not of any particular astrophysical interest; copper is not one of the more abundant metals, and its strong lines lie too far in the ultraviolet to be convenient for observation. It was studied in the present experiment primarily because of all the fairly refractory metals its absolute f-values seem to be the best established.

The f-values of the resonance lines λλ3247 and 3274 were measured by King and Stockbarger[12] using the method of total absorption. They used the vapor pressure equation given by Kelley[13] based on Harteck's data[26] to convert their results to absolute f-values. Hersh[27] has recently redetermined the vapor pressure of copper between 900°C and 1300°C. His results are in good agreement with those of previous investigators and so the vapor pressure of copper may be regarded as fairly well established.

King and Stockbarger's f-values add to give 0.94, which is not too far from 0.81, the sum predicted by Bates Damgaard[5] on the basis of their "modified Coulomb" calculation. The f-values of the Cu I resonance lines should be calculable with some degree of precision. The neutral copper atom in its ground state has the total configuration:

$$(1s^2)(2s^2)(2p^6)(3d^{10})(4s)\ {}^2S_{1/2}.$$

Although the binding of the completed 3d shell is not so great that there will be absolutely no interaction with the single 4s electron; it can be assumed that the wave functions of the low lying states, where none of the 3d electrons are excited, will be fairly well approximated by hydrogen-like wave functions. It would be surprising, therefore, if

a large discrepancy between the measured and calculated f-values were noticed.

Experimentally copper presented no problems. It evaporates readily at temperatures above 1400°C and forms a tough film on a collecting surface. The data on λλ3247 and 3274 are tabulated in Table X. Five plates were taken; 021, 022, and 023, using the "old method" of depositing rate determination; 038 and 039 using the quartz helix.

In reducing the data it was necessary to allow for the hyperfine structure of the copper lines. Each line exhibits hyperfine splitting which is larger than the doppler width of the components but is unresolved by the spectrograph. This hfs splitting was taken into account by considering each line to be composed of two simple components of intensity ratio 5:3. The equivalent widths were divided into two parts in this ratio, the value of C was determined for each part, and these were added to obtain the total C for the line. This is the procedure which was used by King and Stockbarger. The f-values were then calculated in the usual manner.

The f-values were also obtained by the graphical method. Figure 8 shows the experimental data plotted in the same manner as for the other spectra studied. The data for λ3274 were reduced to the same scale as λ3247 using King and Stockbarger's relative f-values for the two lines. The solid line is the copper curve of growth for $\mu = 0.43$, $f_{3247} = 0.38$; the dashed line is the theoretical curve of growth, $\mu = \sin\gamma = 0.62$, $f_{3247} = 0.20$. The "ordinary" curve of growth for copper is included for comparison. The measurements will have to be

extended to include stronger lines before the experimental curve of growth can be drawn with real confidence. This should be particularly easy in the case of copper since the lines are intrinsically very strong.

The results of the present experiment along with those of King and Stockbarger are given in Table IX. As before the values listed under the heading "f(1)" were calculated from the theory, those listed under "f(2)" were found by the graphical method. The sum of the f-values calculated from the theory is 0.32, while the sum of those obtained by the graphical method os 0.58. There seems to be little doubt that the latter values are more nearly correct.

TABLE IX. Cu I ABSOLUTE f-VALUES

Transition		λ	f(K and S[12])	f(1)	f(2)
$4^2S - 4^2P^o$	1/2 - 3/2	3247.54	0.62	0.20	0.38
	1/2 - 1/2	3273.96	0.32	0.12	0.20

TABLE X. Cu I DATA

Plate		$T^{\circ}K$	G	G/QT	$W/\Delta\lambda_D$ λ3247	$W/\Delta\lambda_D$ λ3274
021		1790	0.202	15.6	2.16	1.41
022		1763	0.098	7.72	1.07	0.510
023		1784	0.157	7.45	1.42	0.800
038	(1)	1730	0.0515	2.98	0.74	---
	(2)	1822	0.186	11.6	1.67	0.947
	(3)	1876	0.250	13.3	2.00	1.48
	(4)	1960	0.520	30.5	2.61	2.22
	(5)	1971	0.570	33.1	2.48	2.20
039	(1)	1465	0.042	2.40	0.535	---
	(2)	1505	0.077	4.20	0.726	0.624
	(3)	1555	0.206	11.0	1.52	1.00

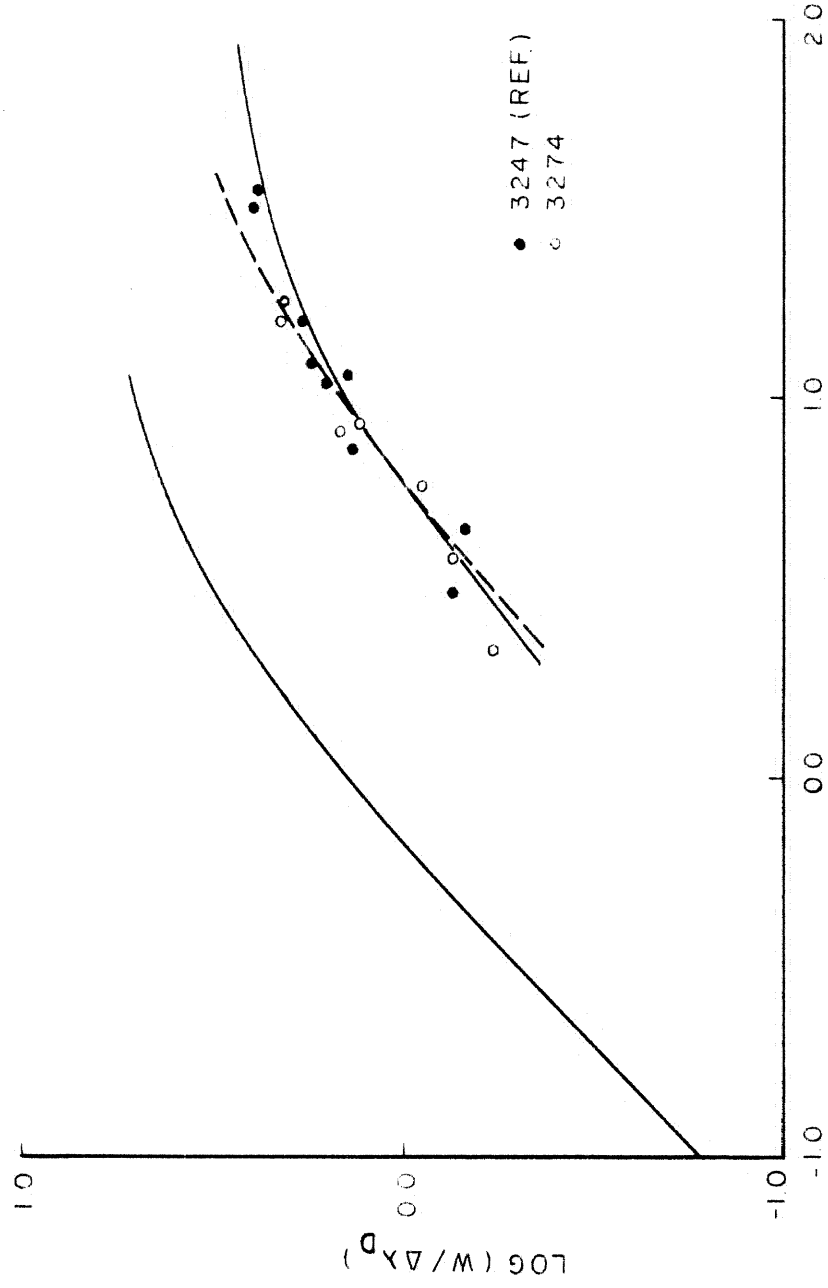

FIG. 8 COPPER

E. Errors

The precision of the final f-values calculated by the theoretical method is limited primarily by uncertainties in the equivalent width measurements. The depositing rates are probably accurate to better than 10 percent, the temperatures to one percent, but the equivalent width measurement may be in error by 20 percent or more. The accuracy improves considerably for stronger lines but the probable error in the equivalent width of any line is probably never less than 10 percent. The uncertainties arise principally from the "grain noise" of the photographic emulsion. A considerable improvement would result if a better means could be devised for performing the required integration over the line contour; or if photographic plates were discarded altogether and a balanced photocell device were used to measure the absorption.

The final f-values, if the theoretical method is taken as correct, all have probable errors of about $\pm$ 15 percent. The graphical method, if justified, involves greater uncertainties and on the basis of the present data the values obtained in this way have probable errors of the order of $\pm$ 30 percent.

V. SUGGESTIONS FOR FURTHER RESEARCH

A. Experimental Techniques

1. Stronger Lines

For all of the spectra studied it would be very desirable to extend the measurements to include stronger lines in order that more accurate experimental curves of growth may be determined. Stronger lines than have been measured up to now should be particularly easy to obtain using copper.

2. Weaker Lines

If a method could be developed whereby equivalent widths of the order of 0.0001 A were measureable (0.002 A is about the smallest that now can be measured with confidence), the work might be extended to include much weaker lines. For certain elements of the iron group, e.g. titanium and vanadium, it may be that only very weak lines can be obtained at all. A new experimental technique may be required if f-values are to be obtained for these elements. It would also be desirable to extend the present measurements to include very weak lines both to establish accurate curves of growth and to measure lines under conditions where molecular effusion must surely occur.

3. Variation in Atomic Beam Geometry

It would be important to carry out a program in which absorption lines are observed with various geometries of the atomic beam; that is with varying widths, with parts of the beam stopped out, etc. Such a program might clear up the problem presented in the present paper, the tendency of the experimental points to establish a curve of growth different from the curve predicted by the theory.

B. Iron Group Elements

1. Scandium

Scandium is neither an abundant element nor does it appear to be a likely prospect for this experiment. Its relative f-values have not been measured.

2. Titanium

Titanium is relatively abundant and is an important element in astrophysics. Relative f-values for a number of the more important lines of the Ti I spectrum were measured by King[28, 29]. Neutral titanium has a complex ground state, a^5F, from which no particularly strong lines arise. Another drawback for the purposes of the present experiment is that it has a very high melting point (1800°C) and temperatures in excess of 2000°C might be required in order to achieve reasonable densities in the atomic beam. Important as they would be, absolute f-values of the Ti I lines do not appear to be determinable by the atomic beam method.

3. Vanadium

Vanadium is also an important element astrophysically and a table of relative f-values is available for lines in its neutral spectrum (King[30]). Unfortunately, the difficulties of high melting point (in this case 1700°C) and complex ground state (a^4F) again may prohibit absolute f-value measurements.

4. Chromium

More data are needed, particularly on strong lines.

5. Manganese

More data are needed.

6. Iron

More data are needed, particularly on strong lines.

7. Cobalt

A program to determine relative f-values for the Co I spectrum has been completed and the results are due to be published soon (Ref. 31). The ground state of the neutral cobalt atom has the configuration a^4F. Two lines were observed on an exploratory plate at 1800°, however, λλ3527 and 3474 (a^4F - z^4F° 9/2 - 9/2, 9/2 - 7/2), so it may prove to be possible to obtain absolute f-values for cobalt by the atomic beam method.

8. Nickel

The relative f-values for many lines in the Ni I spectrum are known from the work of King[32], and Estabrook measured the absolute f-values of the lines λλ3524, 3414, and 3461. There is some evidence that Estabrook's values (Ref. 15) are reliable and it would be of considerable interest to redetermine the absolute f-values of these lines by the atomic beam method. Such a program might prove difficult, however, since the nickel atom has two low lying states, a^3F and a^3D, whose levels overlap to form a complex system of levels. At the temperatures used in the atomic beam experiment the levels from which the lines of interest arise will be relatively depopulated; the atoms will be distributed over all of the low levels in accordance with the Boltzmann distribution. As a result the absorption lines will be weak even if the density of atoms in the atomic beam is high. Moreover, Estabrook's results indicate that the f-values are small, of the order of 0.01.

(9. Copper)

More data are needed on both weak and strong lines.

APPENDIX

VI. ATOMIC BEAM DISTRIBUTION EXPERIMENT

It has already been remarked that the depositing rates obtained for a single run using several mica or aluminum sheets showed considerable scatter among themselves. It was decided that a series of experiments should be conducted to determine whether this scatter resulted from some sort of random variability in the atomic beam, or from something connected with the weighing operation.

Attempts were made to determine the distribution of atoms in the beam by locating six or seven of the sheets over the holes in the upper plate. After a "run" the ratios of the resulting weights to the weight of the central deposit were plotted against the positions of the sheets on the upper plate. The results were compared to the theoretical curve, from Section II-B,

$$G(\xi) = \frac{b^4}{(b^2 + \xi^2)^2} \; G(o).$$

This experiment was repeated using Cr, Cu, and Fe, with mica sheets, aluminum sheets, and glass cover glasses. Although the scatter of the points for a particular run was large, when the results from several runs were averaged the points showed no significant systematic deviation from the theoretical curve.

In an effort to determine the cause of the observed scatter in weights, a long glass plate covering the full spread of the beam was suspended above the source and a thin continuous layer of chromium was deposited. The light transmission through this plate was then determined

as a function of linear distance on the plate, using the microphotometer. The curve obtained was smooth, indicating that the scatter observed in the weight measurements was related to the weighing operation and not to variations in the beam itself. The true beam distribution, however, could not be obtained unambiguously from this light transmission data since it is well known that the relationship between the thickness of a deposited film and its light transmission is not unique but depends upon the depositing rate, the history of the deposited film, etc.

Mr. A. R. Hibbs suggested an experiment by which the distribution of the depositing atoms was directly obtained. 0.1 gram of cobalt enriched with Co^{60} was evaporated from a graphite boat in the usual way. The cobalt deposited on 12 narrow copper strips which were located on a flat plate above the source. As a precaution against radioactive contamination of the apparatus, copper sheets, which were subsequently discarded, were arranged to cover all other area where the beam deposited. In addition the inside of the water jacket was lined with a sheet of molybdenum which was also discarded. The residual pressure in the vacuum chamber was abnormally high during this experiment, of the order of 2×10^{-4} mm-Hg, or about 5 times higher than during actual runs. This was probably due to outgassing of the shields already mentioned.

After the cobalt had evaporated from the boat the copper strips were removed from the vacuum chamber and their gamma-ray activities were measured with a Geiger counter. The original sample of cobalt enriched with Co^{60} had been chosen to give about 10^7 total counts per minute. This activity resulted in a counting rate of the order of 10^4 counts per

minute for the strips located near the center of the beam. The time required for 10^4 counts was determined for each strip and then, taking the activity of the centrally located strip to be unity, the relative activities of the other strips were calculated. The results are shown in Fig. 9 as solid lines whose lengths show the linear distance covered by each strip. The curve shows the predicted beam distribution. The experimentally determined values deviate significantly from the curve for large ξ, but if such a deviation were to exist during a run the effect on the measured f-value would amount to only 2 - 3 percent. Most of the deviation between the experimental values and the theoretical distribution curve can probably be accounted for on the basis of the rather high residual gas pressure in the vacuum chamber. At the pressure which existed during this experiment, 2×10^{-4}mm, roughly 10 percent of the atoms in the beam can be expected to collide with air molecules in flight. This would tend to reduce the density of the deposit near the edges of the beam, corresponding to longer path lengths.

Since the observed deviations from the theoretical beam distribution were small enough to have a negligible effect on the final f-values even if they existed during a run, the Co^{60} experiment was considered to be a confirmation that the density distribution in the atomic beam was adequately given by the theory as developed. The deviation of the results from the expected curves of growth is therefore not explained.

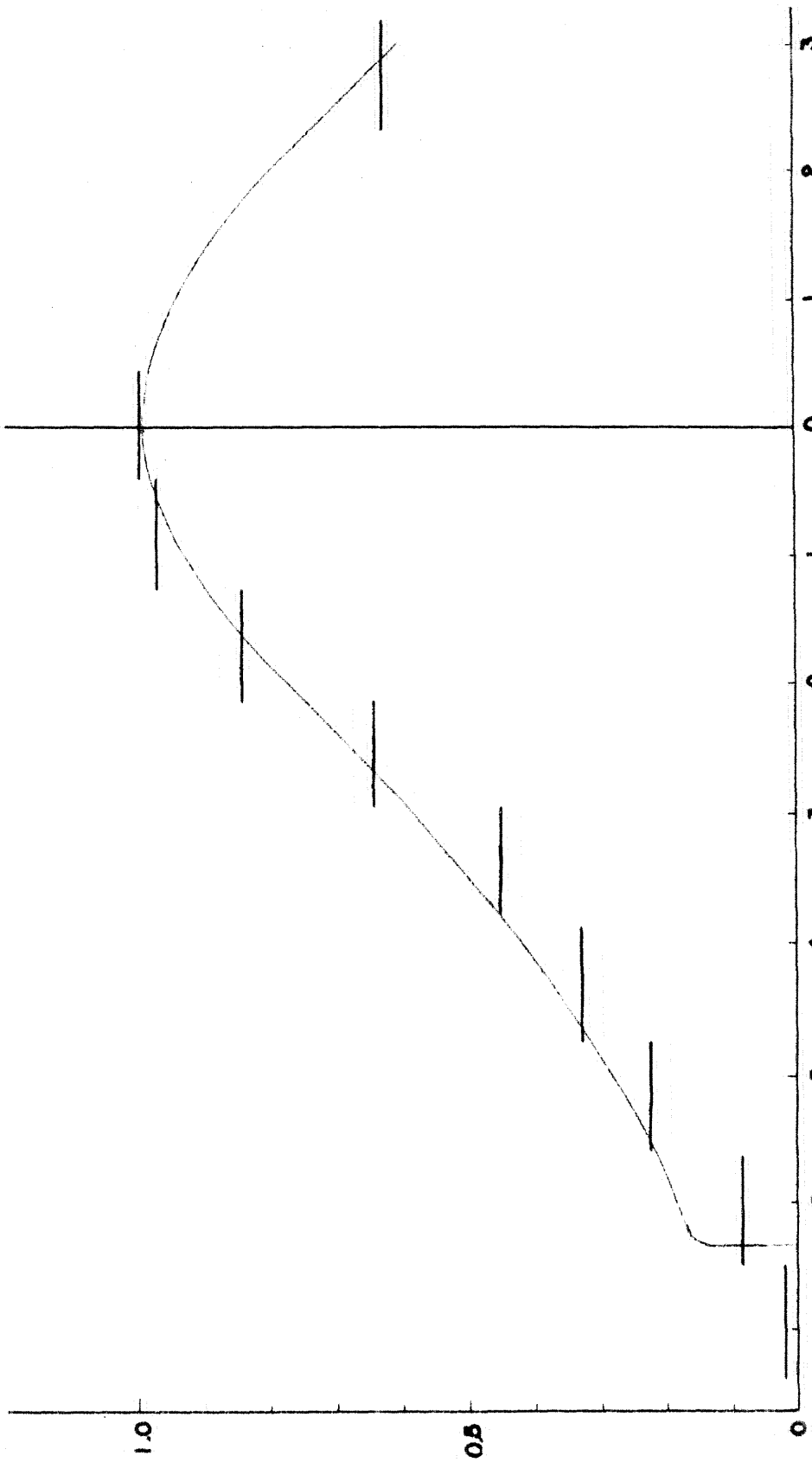

FIG. 9 BEAM DISTRIBUTION

REFERENCES

(1) King, P.B., Astrophys. J. 95, 82 (1942)

(2) Sandage, A.R., and Hill, A.J., Astrophys. J. 113, 525 (1951)

(3) Claas, W.J., Rech. Obs. Utrecht 12, 13 (1951)

(4) Slater, J.C., Quantum Theory of Matter, McGraw-Hill, New York (1951)

(5) Bates, D.R., and Damgaard, A., Phil. Trans. 242A, 101 (1949)

(6) Landolt-Bornstein, Zahlenwerte u. Funktionon, b. 1 Springer, Berlin (1950)

(7) Aller, L.H., Astrophysics, v. 1, Ronald, New York, (1953)

(8) Unsold, A., Z. Astrophys., 24, 306 (1948)

(9) Mitchell, A.C.G., and Zemansky, M., Resonance Radiation and Excited Atoms, Macmillan, New York (1934)

(10) Schuttevaer, J.W., and Smit, J.A., Physica 10, 502 (1943)

(11) King, R.B., and King, A.S., Astrophys. J., 87, 24 (1938)

(12) King, R.B., and Stockberger, D.C., Astrophys. J. 91, 488 (1940)

(13) Kelley, K.K., Bureau of Mines Bull. 350 (1932)

(14) King, R.B., Astrophys. J. 95, 78 (1942)

(15) Estabrook, F.B., Astrophys. J. 113, 684 (1950)

(16) Estabrook, F.B., Astrophys. J., 115, 571L (1952

(17) Kopfermann, H., and Wessel, G., Z. f. Phys. 130, 100 (1951)

(18) Kennard, E.H., Kinetic Theory of Gases, McGraw-Hill, New York (1938)

(19) Hill, A.J., Thesis, Calif. Inst. of Tech. (1950); J. Op. Soc. Am. 41, 315 (1951)

(20) Speiser, R., Johnston, H.L., and Blackburn, P.E., J. Am. Chem. Soc. 72, 4142 (1950)

(21) Gulbransen, E.A., and Andrew, K.F., J. Electrochem. Soc. 99, 402 (1952)

(22) Huldt, L., and Lagerqvist, A., Arkiv for Fysik 5, 91 (1952)

(23) Mack, J.E., Rev. Mod. Phys. 22, 64 (1950)

(24) Carter, W.W., Phys. Rev., 76, 962 (1949)

(25) Marshall, A.L., Dornte, R.W. and Norton, F.J., J. Am. Chem. Soc. 59, 1161 (1937)

(26) Harteck, P., Z. f. Phys.-Chem. 134, 1 (1928)

(27) Hersh, H.N., J. Am. Chem. Soc. 75, 1529 (1953)

(28) King, R.B., and King, A.S., Astrophys. J. 87, 359 (1938)

(29) King, R.B., Astrophys. J. 94, 425 (1941)

(30) King, R.B., Astrophys. J. 105, 467 (1947)

(31) King, R.B. (to be published)

(32) King, R.B., Astrophys. J. 108, 203 (1948)

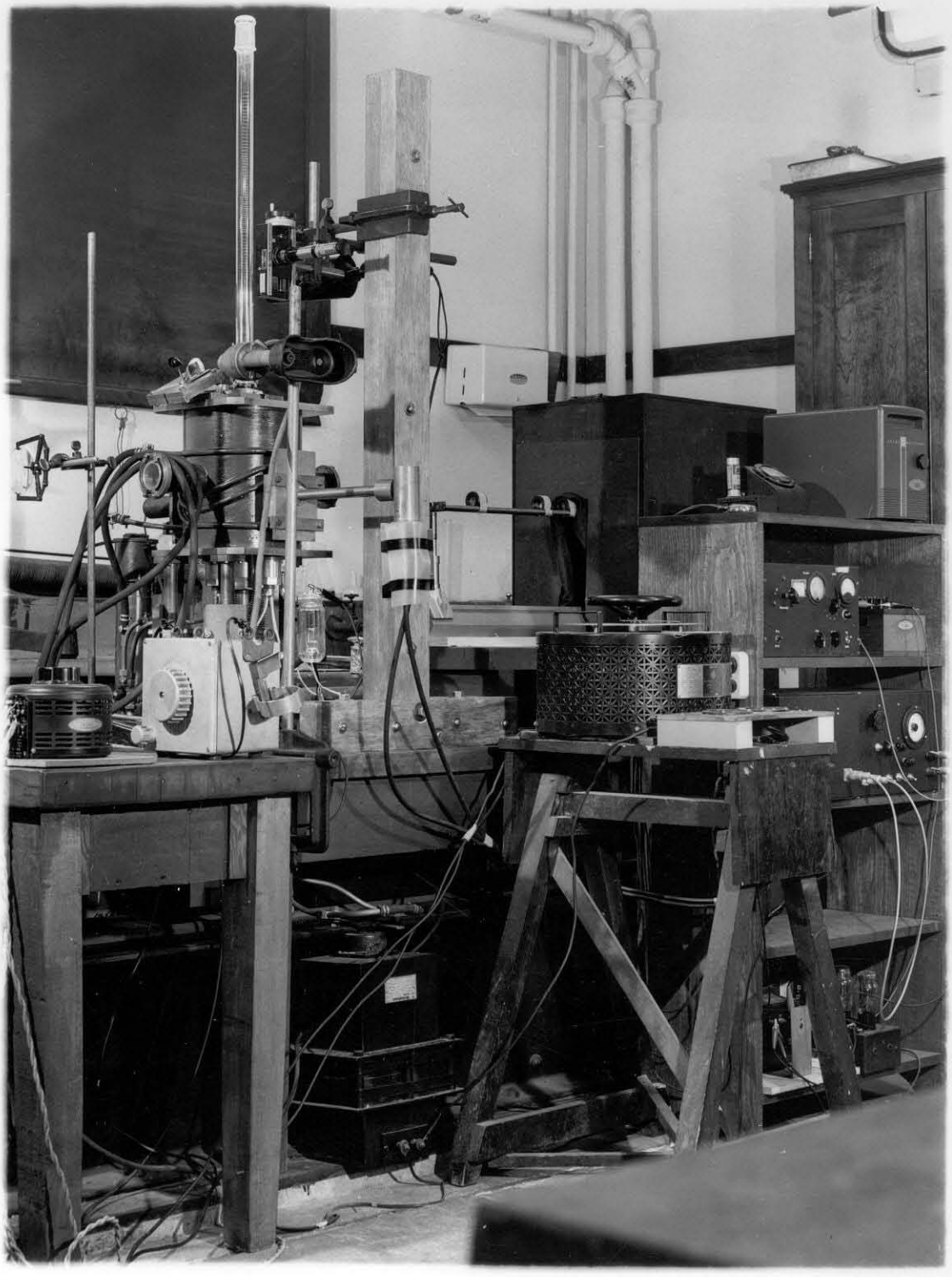

FIG. 10